Norconsult

NOTAT

Norconsult AS | Valkendorfsgate 6, NO-5012 Bergen | Pb. 1199, NO-5811 Bergen

Tel: +47 55 37 55 00 | Fax: +47 55 37 55 01

Notat nr.: 1

Oppdragsnr.: 5142646

Notat: Utredning av høye rekkverk på Askøybrua

Vedlegg 4:

Rapport: Askøy bridge, Wind tunnel tests and analyses, Desember 2014.

Vedlegg C tilkom i januar 2015.

Svend Ole Hansen APS.

Svend Ole Hansen ApS

SCT. JØRGENS ALLÉ 5C · DK-1615 KØBENHAVN V · DENMARK
TEL: (+45) 33 25 38 38 · WWW.SOHANSEN.DK

WIND
ENGINEERING
FLUID
DYNAMICS

ASKØY BRIDGE

Wind tunnel tests and analyses

Carried out for: Statens vegvesen

Revision 0, December 2014

CONTENTS

Contents – Annex

REVISIONS

Revision no.	Date of issue	Comments
0	December 19, 2014	Report draft for comments. Flutter derivatives not included.

Copenhagen, December 19, 2014

Svend Ole Hansen ApS   Project engineer   Project engineer

Svend Ole Hansen   Robin George Srouji   Adam Andersen Læssøe

0 Summary and conclusion

The present report describes the wind tunnel tests investigating Askøy Bridge. All structural data for the section models such as geometry, mass, mode shapes and corresponding natural frequencies simulated in the wind tunnel tests, have been based on information received from Statens vegvesen.

0.1 Summary

The wind tunnel tests investigate the bridge with the present railings, new railings and with one and two walkways, respectively. Both types of railing are tested in the in-service state without traffic. Two different types of measurements have been conducted:

- Static section model tests for determination of static load coefficients for drag, lift and moment.
- Dynamic section model tests for simulation of the vertical and torsional vibrations of the bridge induced by vortex shedding and buffeting.

Vortex-induced vibrations are investigated in low turbulent flow, i.e. flow with a turbulence intensity below 1%. In low turbulent flow, negligible turbulence fluctuations occur at very high frequencies. These turbulence fluctuations may amplify vortex-induced vibrations, indicating that the results obtained may overestimate the response. The test results obtained for vertical and torsional vortex-induced vibrations may be used to predict the full scale behaviour of all relevant vertical and torsional modes, respectively.

0.2 Main conclusions

The tests show that the bridge cross section is not susceptible to vertical vortex-induced vibrations for logarithmic damping decrements above approx. 3.6% for heaving vibrations and 1.8% for torsional vibrations. For lower damping, vortex-induced vibrations might occur for some configurations both in heave and torsion.

0.3 Static load coefficients – main results

Table 0.2 shows the main results of the static load coefficients measured on the section models.

Table 0.2. Static load coefficients for measurements in static wind tunnel tests at an incidence angle of 0° (the numeric largest value in the range from -1.5° to 1.5° is shown - where both positive and negative values occur, both are shown). The slopes $dC_L/d\alpha$ and $dC_M/d\alpha$ are determined as the numerically largest slope of a fitted second-degree polynomial in the interval -3° to 3°. See further results in Annex B.

Config.	Bridge configuration	Drag, C_D	Lift, C_L	$dC_L/d\alpha$	Moment, C_M	$dC_M/d\alpha$
1	Present bridge.	0.536	-0.329	5.632	-0.042/0.038	1.749
2a	One walkway upstream.	0.699	-0.341	6.471	-0.025/0.137	3.154
2c	One walkway upstream, guide vanes.	0.736	-0.440	4.981	-0.040/0.094	2.582
3	Present bridge, modified railings.	0.661	-0.461	5.464	-0.064/0.027	1.726

| 4 | Two walkways. | | | 0.718 | -0.412 | 6.669 | -0.016/0.128 | 2.965 |

0.4 Vortex-induced vibrations – main results

Table 0.4 and Table 0.5 show the general mass-damping parameter of the section model together with the dynamic properties of vertical and torsional vortex-induced vibrations of the bridge deck, respectively.

Table 0.4: Dynamic properties for vertical (heaving) vortex-induced vibrations and general mass-damping parameters of the section models. Further results may be seen in Annex D.

Config.	Bridge configuration	δ [% LD]	$Sc_{G,H}$ [-]	Vortex-induced vibrations	$U_{crit,FS}$ [m/s]	St [-]	r/h [-]	$a_{FS,H}$ [m/s²]
1	Present bridge.	0.8	2.59	Yes	4.02	0.13	0.055	0.21
1	Present bridge.	2.0	6.24	Yes	3.35	0.16	0.019	0.07
1	Present bridge.	3.6	11.7	No	-	-	-	-
2a	One walkway upstream.	1.7	5.57	Yes	5.27	0.10	0.061	0.23
2a	One walkway upstream.	2.6	9.40	No	-	-	-	-
2a	One walkway upstream.	3.6	12.5	No	-	-	-	-
2b	One walkway downstream.	1.6	5.47	No	-	-	-	-
2c	One walkway upstream, guide vanes.	1.9	6.62	Yes	6.17	0.09	0.076	0.29
2d	One walkway upstream, guide vanes, vortex spoiler.	1.9	6.62	Yes	6.77	0.08	0.039	0.15
3	Present bridge, modified railings.	0.8	2.59	Yes	4.01	0.13	0.063	0.24
3	Present bridge, modified railings.	1.9	5.93	Yes	4.08	0.13	0.018	0.07
3	Present bridge, modified railings.	3.6	11.7	No	-	-	-	-
4	Two walkways.	1.9	6.41	No	-	-	-	-

Table 0.5: Dynamic properties for torsional vortex-induced vibrations and general mass-damping parameters of the section models and the full scale structure. The full-scale acceleration a_{FS} refer to the outer bridge deck edge vibrations. Further results may be seen in Annex D.

Config.	Bridge configuration	δ [% LD]	$Sc_{G,T}$ [-]	Vortex-induced vibrations	$U_{crit,FS}$ [m/s]	St [-]	Φ [°]	$a_{FS,T}$ [m/s²]
1	Present bridge.	0.6	0.99	Yes	14.7	0.12	1.04	1.81
1	Present bridge.	1.8	3.00	No	-	-	-	-
2a	One walkway upstream.	0.8	1.96	Yes	13.9	0.11	0.30	0.41
2b	One walkway downstream.	1.1	2.86	No	-	-	-	-
2d	One walkway upstream, guide vanes, vortex spoiler.	0.9	2.34	Yes	17.9	0.08	0.30	0.40
3	Present bridge, modified railings.	0.7	1.17	Yes	15.3	0.11	0.64	1.10

3	Present bridge, modified railings.	1.1	1.85	Yes	14.9	0.11	0.19	0.32
3	Present bridge, modified railings.	1.5	2.53	No	-	-	-	-
4	Two walkways.	1.4	3.48	No	-	-	-	-

The tests show that the bridge cross section is not susceptible to vertical vortex-induced vibrations for logarithmic damping decrements above approx. 3.6% for heaving vibrations and 1.8% for torsional vibrations. For lower damping, vortex-induced vibrations might for some configurations occur both in heave and torsion.

At the critical wind velocity, the present bridge (configuration 1) vibrates resonantly and a peak full scale acceleration of 1.81 m/s^2 or 0.18g at the outer edge of the bridge deck is observed for torsional vibrations with a logarithmic damping decrement of 0.6%. In comparison, the bridge deck with modified railings (configuration 3) has a peak full scale acceleration of 1.10 m/s^2 or 0.11g at the outer edge of the bridge deck with a damping of 0.7% while the configuration with one walkway (configuration 2) and two walkways (configuration 4) have a peak full scale acceleration of 0.41 m/s^2 or 0.04g and nothing at all with a damping of 0.8% and 1.4%, respectively. For higher vertical and torsional modes, the critical wind velocity and accelerations will be larger.

Aerodynamic modifications in terms of guide vanes did not reduce the vortex-induced vibrations. Adding a vortex spoiler along with guide vanes do, however, reduce the heaving vibrations from 0.23 m/s^2 for configuration 2a to 0.15 m/s^2. The guide vanes and vortex spoiler have no influence on the torsional vibrations.

1 Introduction

The present report describes the wind tunnel tests investigating Askøy Bridge. All structural data for the section model such as geometry, mass, mode shapes and corresponding natural frequencies simulated in the wind tunnel tests, have been based on information received from Statens vegvesen.

The Askøy Bridge is a suspension bridge with a main span of 850 m. The cross-section consists of a simple 15.5 m wide composite deck. One or two walkways may be attached to the deck, increasing the total width to 18.5 m and 21.5 m, respectively. The height of the cross-section at the outer edges is approx. 3 m. The deck is supported by two pylons, see Figure 1.1.

The wind tunnel tests investigate the bridge with the present railings, new railings and with one and two walkways, respectively. Both types of railing are tested in the in-service state without traffic. Two different types of measurements have been conducted:

- Static section model tests for determination of static load coefficients for drag, lift and moment.
- Dynamic section model tests for simulation of the vertical and torsional vibrations of the bridge induced by vortex shedding and buffeting.

The models investigated and the test arrangements are described in chapter 2 and 3, respectively. A further description of the wind tunnel is found in Annex E. The results are available in chapter 4-6 and in Annex B-D. The theory behind the calculations is described in Annex A.

The main objectives of the wind tunnel tests are to determine non-dimensional wind action parameters used to estimate the bridge behaviour in natural wind. These wind action parameters consist of static load coefficients and wind action parameters describing the susceptibility to buffeting- and vortex-induced vibrations.
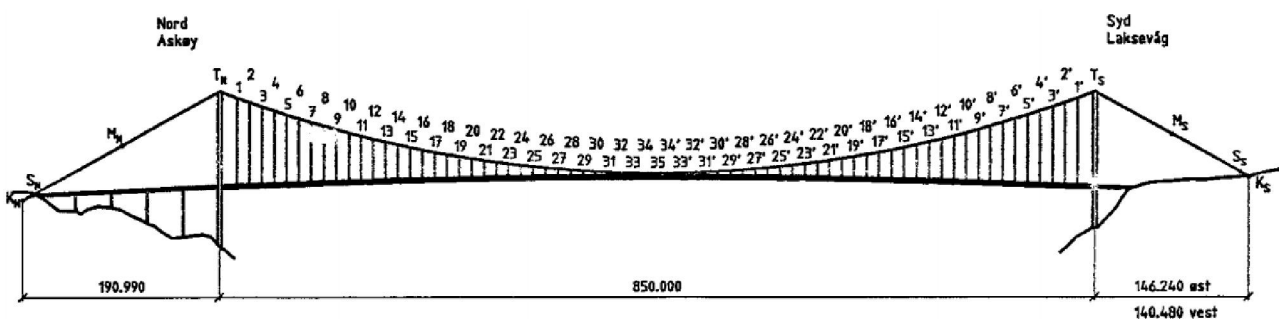
Figure 1.1: Askøy Bridge.

The basis of the wind tunnel tests carried out consists of geometrical information and information on modal vibrations and is listed below.

1.1 Basis of wind tunnel tests

All structural data for the wind tunnel model such as geometry, mass, mode shapes and corresponding natural frequencies simulated in the wind tunnel tests carried out, have been based on information received from Statens vegvesen.

The following information has been received:

E-mail on 09.08.2014:   *Gangbane Askøybrua rev01.pdf*

K100.pdf, K1101.pdf, K110.pdf, K112.pdf, K114.pdf, K116.pdf

Som bygget tegninger Askøybrua.pdf

Tegningsblad 8.04 fra 1994.pdf

Tegningsblad 8.08 fra 1994.pdf

E-mail on 09.18.2014:   *Gangbane Askøybrua rev02.pdf*

K100.pdf

K101.pdf

E-mail on 09.26.2014:   *3320_001.pdf*

E-mail on 10.03.2014:   *Gangbane Askøybrua rev03.pdf*

The information on which the wind tunnel tests are based can be found in Annex F. Drawings are not included.

1.2 Limitations

The results presented in the report regarding buffeting (to be included in revision 1) and vortex-induced vibrations are directly applicable to a full scale structure with geometry, frequency ratio, mode shapes, damping, modal mass etc. equivalent to those of the model.

2 Model setup

The wind tunnel tests are carried out with a section model of the Askøy Bridge. The model is described below. Model details such as the railings are modelled as detailed as possible. For the cylindrical parts of the railings, the non-matching Reynolds numbers have not been considered a source of gross errors.

2.1   Section model

The length of the section models are 1.7 m. The cross section actually modelled is shown in Figure 2.1. The model scale is 1:50. The mass of the model is reported in the annexes, where relevant for the test results.
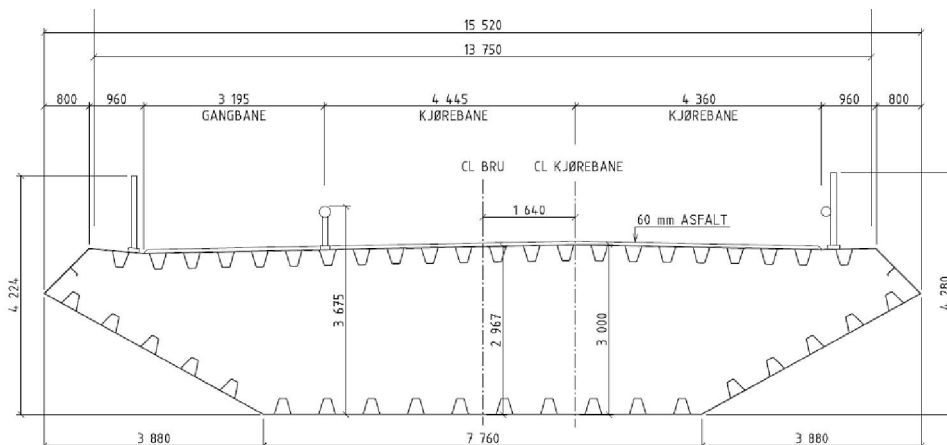
Figure 2.1: General cross section of the Askøy Bridge section model. Dimensions are in full scale [mm].

The bridge deck is modelled as a stiff model with a low weight allowing extra mass to be added when mass scaling and natural frequencies are set. The railings are 3D printed.

3 Test arrangements

Static and dynamic tests with the section models have been carried out in the wind tunnel.

3.1   Section model setup

Static tests are carried out to determine load coefficients and dynamic tests are carried out to investigate vibrations caused by vortex-induced vibrations and buffeting.

Static test setup:

- See principal sketch in Figure 3.1. The rigs are connected to force transducers by stiff wires.

Dynamic test setup:

- See principal sketch in Figure 3.1. The rigs are connected to force transducers by springs. Hence, the model is responding in a mode shape close to uniform.
- Additional mass can be mounted on the rigs and the position of the force transducers and springs may be adjusted in order to achieve target natural frequencies, mass and mass moment of inertia.
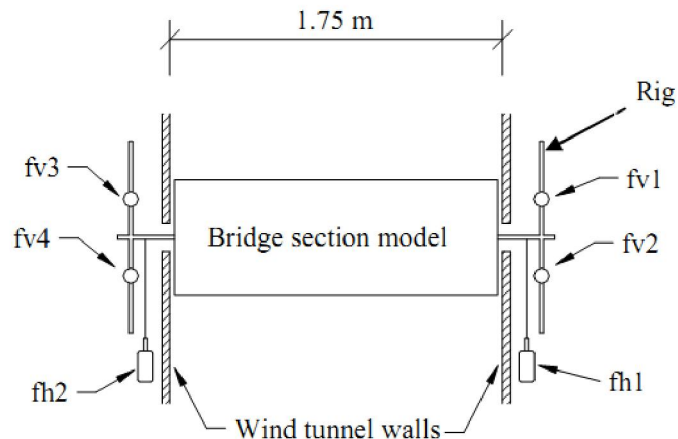
Figure 3.1: Plan view of test setup of section models. Four force transducers fv1, fv2, fv3 and fv4 measure forces/translations in the vertical direction. Two force transducers fh1 and fh2 measure forces/translations in the horizontal direction. In the dynamic tests, the transducers are connected to the model by springs. In the static tests, the transducers and the model are connected by stiff wires.

The configurations listed below have been modelled of the bridge deck. The tested configurations for each test type will be presented in their respective chapter.

- Configuration 1: Present bridge.
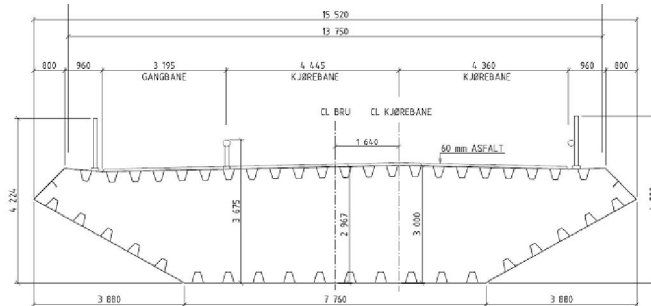
Figure 3.2: Present bridge.

- Configuration 2a, 2b, 2c, and 2d: One walkway upstream (2a) or downstream (2b) with guide vanes positioned on the lower edges of the bridge section (2c) and vortex spoiler positioned on centrally on underside (2d). In configurations 2c and 2d the walkway is positioned upstream.
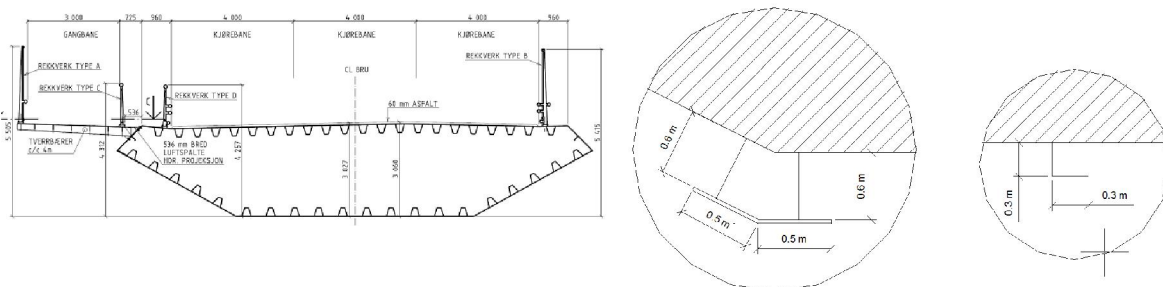
Figure 3.3: Right: Bridge deck with one walkway attached. Left: Guide vanes and vortex spoiler, respectively. Both are placed beneath the bridge deck. The vortex spoiler is located at the centre.

- Configuration 3: Present bridge with modified railings.
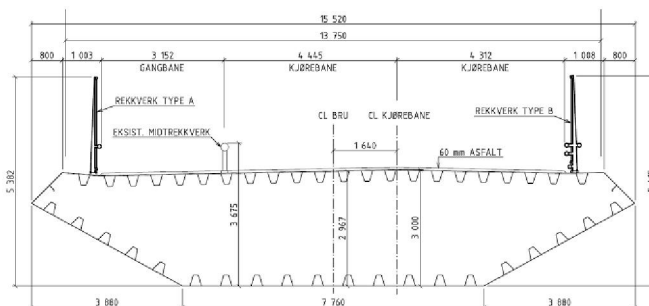
Figure 3.4: Present bridge with modified railings.

- Configuration 4: Two walkways.
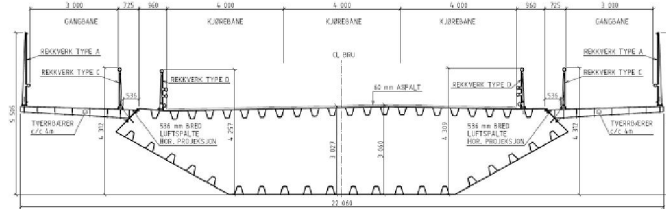
Figure 3.5: Bridge deck with two walkways attached.

The response of the section model is measured with six force transducers of the type Hottinger, Z6-2/D1. Two transducers measure the drag acting on the model and four transducers measure the lift and torsional moment acting on the model. The force transducers are calibrated by suspending masses from the transducers. The calibration has been undertaken individually for each horizontal transducer and for all vertical transducers in one by putting known weight on the bridge section model.

3.2   Other instrumentation

The flow is measured with a Pitot tube connected to a manometer. In order to determine the flow velocity from the measured velocity pressure, the temperature, barometric pressure and humidity is measured as well. All instrumentation used to determine the flow velocity is calibrated every year at external accredited institutions.

All signals are collected on a computer with data acquisition equipment and software. In all tests, the data have been collected using a sample frequency of 500 Hz.

Table 3.1. Instrumentation used in the wind tunnel testing.

Wind tunnel instrumentation
Hottinger, Z6-2/D1. Six transducers.
PT100 temperature sensor, wind tunnel.
PT100 temperature sensor, control room.
PPC500 Furness pressure calibrator.
HMW71U Humidity transmitter.
PTB100AVaisala analogue barometer.
Dantec hot-wire system used to measure fluctuating wind velocities.
Pitot tube.
Computer Board. 16 bit A/D data acquisition board.
PC dedicated to data acquisition.

4 Load coefficients – section model

Static tests have been carried out in order to determine load coefficients.

4.1 Measurements

Load coefficients for drag, lift and overturning moment are measured with a static test setup on the section model of the Askøy Bridge. The configurations shown in Table 4.1 have been tested.

Table 4.1: Tested configurations. All configurations have been tested in turbulent flow with a turbulence intensity of approx. 13-15%.

Config.	Bridge configuration	Angle [°]	Figure
1	Present bridge.	0, ±1.5, ±3, ±4, ±6, ±8, ±10	B.2
2a	One walkway upstream.	0, ±1.5, ±3, ±4, ±6, ±8, ±10	B.3
2c	One walkway upstream, guide vanes.	0, ±1.5, ±3, ±4, ±6, ±8, ±10	B.4
3	Present bridge with modified railings.	0, ±1.5, ±3, ±4, ±6, ±8, ±10	B.5
4	Two walkways.	0, ±1.5, ±3, ±4, ±6, ±8, ±10	B.6

The tests are carried out at a wind tunnel air velocity of approx. 6 m/s with a measuring time of 60 s.

The measurements carried out include drag C_D in the wind direction, lift C_L perpendicular to the wind direction and the overturning moment C_M. The mean drag, lift and moment load per unit length acting on bridge decks is determined as:

Drag:
$$F_D(z) = q_m(z)hC_D \tag{4.1}$$

Lift:
$$F_L(z) = q_m(z)bC_L \tag{4.2}$$

Moment:
$$F_M(z) = q_m(z)b^2C_M \tag{4.3}$$

where

b is the along-wind dimension of the structural part considered. Here the width of the bridge cross section ($b = 15.5$ m).

h is the cross-wind dimension of the structural part considered. Here the height of the bridge cross section ($h = 3.00$ m).

C_D, C_L, C_M are the drag, lift and moment coefficient, respectively.

$q_m(z)$ is the mean velocity pressure at height z defined by:

$$q(z) = \frac{1}{2}\rho_{air}U^2 \tag{4.4}$$

where ρ_{air} is the air density and U is the time averaged wind velocity.

The definition of the load directions are shown in Figure 4.1.
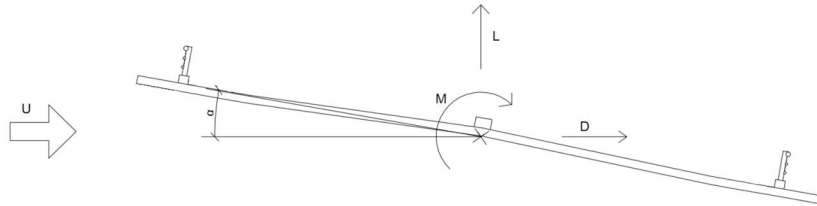
Figure 4.1: Principle sketch of the definition of the incidence angle and wind loads acting on the bridge deck. The shown rotation corresponds to a positive torsional angle.

4.2 Results

The results of the measurements of static load coefficients are shown in Annex B. Main results are shown in Table 4.2.

Table 4.2: Static load coefficients for measurements in static wind tunnel tests at an incidence angle of 0° (the numeric largest value in the range from -1.5° to 1.5° is shown - where both positive and negative values occur, both are shown). The slopes $dC_L/d\alpha$ and $dC_M/d\alpha$ are determined as the numerically largest slope of a fitted second-degree polynomial in the interval -3° to 3°. See further results in Annex B.

Config.	Drag, C_D	Lift, C_L	$dC_L/d\alpha$	Moment, C_M	$dC_M/d\alpha$
1	0.536	-0.329	5.632	-0.042/0.038	1.749
2a	0.699	-0.341	6.471	-0.025/0.137	3.154
2b	0.736	-0.440	4.981	-0.040/0.094	2.582
3	0.661	-0.461	5.464	-0.064/0.027	1.726
4	0.718	-0.412	6.669	-0.016/0.128	2.965

5 Buffeting-induced vibrations – section model

Tests with buffeting-induced vibrations are carried out on a section model of the Askøy Bridge in the dynamic test setup.

5.1 Theory

Buffeting tests have been carried out for the Askøy Bridge cross sections. Any galloping response will also appear in the tests, however, no distinction is made between buffeting and galloping response. The tests include both buffeting response and investigation of critical flutter wind speeds.

In order to simulate critical flutter velocities correctly, the frequency ratio of the torsional and vertical natural frequencies is important. The sensitivity of coupling of a vertical and torsional mode shape is dependent on the magnitude of the two natural frequencies and their internal frequency ratio. The higher natural frequencies and frequency ratio, the higher critical flutter velocities.

The sensitivity also highly depends on the mode coupling coefficient $C_\xi C_\alpha$, which is defined by:

$$C_\xi = \int^{deck} \xi(x)\alpha(x)\,dx \Big/ \int^{deck} \xi^2(x)\,dx \tag{5.1}$$

$$C_\alpha = \int^{deck} \xi(x)\alpha(x)\,dx \Big/ \int^{deck} \alpha^2(x)\,dx \tag{5.2}$$

where α and ξ are the torsional (along the bridge deck axis) and vertical mode shape.

Similar vertical and torsional mode shapes, i.e. $C_\xi C_\alpha = 1$, indicates possible mode coupling. If $C_\xi C_\alpha = 0$ the mode shapes are not likely to couple. In the wind tunnel tests with section models both the vertical and torsional mode shapes have constant amplitude providing $C_\xi C_\alpha = 1$. Hence, the wind tunnel tests with section models will provide conservative results when the investigated mode shapes have mode coupling coefficient $C_\xi C_\alpha < 1$, see [3].

The full scale wind speeds are determined from the following:

$$\left(\frac{n_H b}{U}\right)_{model} = \left(\frac{n_H b}{U}\right)_{full-scale} \tag{5.3}$$

where

n_H is the vertical frequency.

U is the wind speed.

5.2 Measurements

Measurements and results will be included in revision 1.

6 Flutter derivatives

The flutter derivatives will be included in revision 1.

7 Vortex-induced vibrations – section model

Tests with vortex-induced vibrations are carried out on section models of the Askøy Bridge in the dynamic test setup.

7.1 Theory

The present section summarizes the theory used to determine vortex-induced vibrations of the bridge sections. For further explanation regarding the theory presented in this section see Annex A.

Vortices are shed from side to side with a vortex shedding frequency n_s determined by:

$$n_s = St \frac{U}{h} \tag{6.1}$$

where

St	is the Strouhal number.
U	is the mean wind speed.
h	is the height of the bridge deck.

The critical wind speed U_{crit} occurs when the vortex-shedding frequency is equal to the natural frequency, i.e. $n_s = n_e$:

$$U_{crit} = \frac{1}{St} h \, n_e \tag{6.2}$$

The sensitivity of the bridge deck to vortex-induced vibrations may be evaluated by the general mass-damping parameter Sc_G, which includes the model's width b, mass per unit length m_e and the mass moment of inertia per unit length I_e:

Bending: $$Sc_{G,H} = \frac{2\delta_s m_e}{\rho_{air} hb} \tag{6.3}$$

Torsion: $$Sc_{G,t} = \frac{2\delta_s I_e}{\rho_{air} h^2 b^2} \tag{6.4}$$

The standard deviation of the vortex-induced structural deflection $\sigma_{y,max}$ at the point where the mode shape $\xi(z)$ has its largest deflection $\sigma_{y,max}$ is given by:

$$\frac{\sigma_{y,max}}{h} = \frac{1}{St^2} \frac{C_c}{\sqrt{\frac{Sc_G}{4\pi} - K_{aG}\left(1 - \left(\frac{\sigma_{y,max}}{a_L h}\right)^2\right)}} \sqrt{\frac{\rho hb}{m_e}} \sqrt{\frac{h}{l}} \tag{6.5}$$

where

C_c	is an aerodynamic constant giving vibration amplitudes at high Sc_G.
K_a	is an aerodynamic damping factor.

a_L is the limit of the vibration of the structure with a very small damping.

l is the length of the bridge.

C_c, K_{aG} and a_L all depend on Reynolds number.

7.2 Measurements

The expression of the general mass-damping parameter Sc_G shows that mass scaling and the structural damping are crucial parameters. In the tests, the effective mass of the wind tunnel model is fitted to the full scale mass, while the structural damping is set as low as possible in order to determine the resonance air velocity and show the cross section's susceptibility to vortex shedding.

The bridge section model has been tested in low turbulent flow where the bridge is most sensitive to vortex-induced vibrations. Seven configurations have been tested, see Table 6.1. The tests have been carried out for full scale wind speeds up to approx. 30 m/s.

Table 6.1: Investigated configurations for vortex-induced vibrations. All configurations have been tested in low turbulent flow.

Config.	Bridge configuration	Figure
1	Present bridge.	D.1-D.5
2a	One walkway upstream.	D.6-D.10
2b	One walkway downstream.	D.11-D.12
2c	One walkway upstream, guide vanes.	D.13
2d	One walkway upstream, guide vanes, vortex spoiler.	D.14-D.15
3	Present bridge, modified railings.	D.16-D.21
4	Two walkways.	D.22-D.23

In order to translate the data from tables and plots in the following pages, the frequencies and normalisation height are needed. These are listed in Table 6.2 for the full scale structure.

Table 6.2: Vertical frequency n_H, torsional frequency n_T, and normalisation height h of full scale structure.

Config.	n_H [Hz]	n_T [Hz]	h [m]
1, 3	0.18	0.57	3.00
2a, 2b, 4	0.18	0.50	3.00

7.3 Results

The test results for vortex-induced vibrations are documented in Annex D. The results are presented as function of the normalised wind speed.

Table 6.3 and Table 6.4 show the general mass-damping parameter of the section models together with the dynamic properties of vertical and torsional vortex-induced vibrations of the bridge deck, respectively.

Table 6.3: Dynamic properties for vertical vortex-induced vibrations and general mass-damping parameters of the section models. The full-scale acceleration a_{FS} refer to vibrations with the vertical frequency given in Table 6.2. Further results may be seen in Annex D.

Config.	Bridge configuration	δ [% LD]	$Sc_{G,H}$ [-]	Vortex-induced vibrations	$U_{crit,FS}$ [m/s]	St [-]	r/h [-]	$a_{FS,H}$ [m/s²]
1	Present bridge.	0.8	2.59	Yes	4.02	0.13	0.055	0.21
1	Present bridge.	2.0	6.24	Yes	3.35	0.16	0.019	0.07
1	Present bridge.	3.6	11.7	No	-	-	-	-
2a	One walkway upstream.	1.7	5.57	Yes	5.27	0.10	0.061	0.23
2a	One walkway upstream.	2.6	9.40	No	-	-	-	-
2a	One walkway upstream.	3.6	12.5	No	-	-	-	-
2b	One walkway downstream.	1.6	5.47	No	-	-	-	-
2c	One walkway upstream, guide vanes.	1.9	6.62	Yes	6.17	0.09	0.076	0.29
2d	One walkway upstream, guide vanes, vortex spoiler.	1.9	6.62	Yes	6.77	0.08	0.039	0.15
3	Present bridge, modified railings.	0.8	2.59	Yes	4.01	0.13	0.063	0.24
3	Present bridge, modified railings.	1.9	5.93	Yes	4.08	0.13	0.018	0.07
3	Present bridge, modified railings.	3.6	11.7	No	-	-	-	-
4	Two walkways.	1.9	6.41	No	-	-	-	-

Table 6.4: Dynamic properties for torsional vortex-induced vibrations and general mass-damping parameters of the section models. The full-scale acceleration a_{FS} refer to the outer bridge deck edge vibrations with the torsional frequency given in Table 6.2. Further results may be seen in Annex D.

Config.	Bridge configuration	δ [% LD]	$Sc_{G,T}$ [-]	Vortex-induced vibrations	$U_{crit,FS}$ [m/s]	St [-]	Φ [°]	$a_{FS,T}$ [m/s²]
1	Present bridge.	0.6	0.99	Yes	14.7	0.12	1.04	1.81
1	Present bridge.	1.8	3.00	No	-	-	-	-
2a	One walkway upstream.	0.8	1.96	Yes	13.9	0.11	0.30	0.41
2b	One walkway downstream.	1.1	2.86	No	-	-	-	-
2d	One walkway upstream, guide vanes, vortex spoiler.	0.9	2.34	Yes	17.9	0.08	0.30	0.40
3	Present bridge, modified railings.	0.7	1.17	Yes	15.3	0.11	0.64	1.10
3	Present bridge, modified railings.	1.1	1.85	Yes	14.9	0.11	0.19	0.32
3	Present bridge, modified railings.	1.5	2.53	No	-	-	-	-
4	Two walkways.	1.4	3.48	No	-	-	-	-

The tests show that the bridge cross section is not susceptible to vertical vortex-induced vibrations for logarithmic damping decrements above approx. 3.6% for heaving vibrations and 1.8% for torsional vibrations. For lower damping, vortex-induced vibrations might for some configurations occur both in heave and torsion, see e.g. Figure 6.1 and Figure 6.2 for configuration 1 (present bridge).

In general, aerodynamic deck sections with open railings will not be vulnerable to vortex-induced vibrations. The railings will tend to break up the vortex shedding and cause a lack of synchronicity between the vortices at different positions along the bridge deck length axis, while the aerodynamic deck section will give a streamlined shape.

The critical velocity for all the configurations lie within full scale wind velocities of 3.4-6.8 m/s and 13.9-17.9 m/s for heaving and torsional vibrations, respectively. Such wind velocities are not quite high enough to provide significant turbulence in the wind, which would reduce the vibration amplitudes.

At the critical wind velocity, the present bridge (configuration 1) vibrates resonantly and a peak full scale acceleration of 1.81 m/s^2 or 0.18g at the outer edge of the bridge deck is observed for torsional vibrations with a logarithmic damping decrement of 0.6%. In comparison, the bridge deck with modified railings (configuration 3) has a peak full scale acceleration of 1.10 m/s^2 or 0.11g at the outer edge of the bridge deck with a damping of 0.7% while the configuration with one walkway (configuration 2) and two walkways (configuration 4) have a peak full scale acceleration of 0.41 m/s^2 or 0.04g and nothing at all with a damping of 0.8% and 1.4%, respectively. For higher vertical and torsional modes, the critical wind velocity and accelerations will be larger.

Figure 6.1: Vortex-induced vibrations of configuration 1 (present bridge) with a logarithmic damping decrement of approx. 0.8%. Parameters to convert into full scale vibrations may be found in Table 6.2. The wind velocity is normalised with the height of the bridge deck corresponding to 3.00 m in full scale and the vertical frequency in still air. In order to get full scale wind velocities, the normalised wind velocity is multiplied by the full scale vertical frequency and height of the bridge deck.
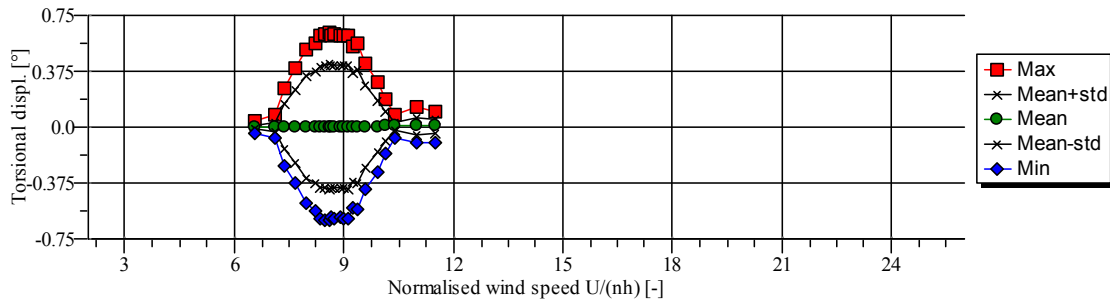
Figure 6.2: Vortex-induced vibrations of configuration 1 (present bridge) with a logarithmic damping decrement of approx. 0.6 %. Parameters to convert into full scale vibrations can be found in Table 6.2. The wind velocity is normalised with the height of the bridge deck corresponding to 3.00 m in full scale and the torsional frequency in still air. In order to get full scale wind velocities, the normalised wind velocity is multiplied by the full scale torsional frequency and height of the bridge deck.

Aerodynamic modifications in terms of guide vanes did not reduce the vortex-induced vibrations. Adding a vortex spoiler along with guide vanes do, however, reduce the heaving vibrations from 0.23 m/s² for configuration 2a to 0.15 m/s². The guide vanes and vortex spoiler have no influence on the torsional vibrations.

8   References

[1] Hansen, S. O.: *Vortex-induced and galloping-induced vibrations of simple structures*. ICWE13, July 2011. Amsterdam, Netherlands.

[2] Hansen, S. O.: *Vortex-induced vibrations – the Scruton number revisited*. Accepted for publication at the institute of Civil Engineers, Structural and Buildings Journal.

[3] Dyrbye, C. and Hansen, S.O.: *Wind Loads on Structures*, John Wiley & Sons, (1997)

[4] Dansk Standard, Eurocode 1: *Last på bærende konstruktioner - Del 1-4: Generelle laster - Vindlast*, Dansk Standard, 2007.

[5] Sumer, B. M. and Fredsøe, J.: *Hydrodynamics Around Cylindrical Structures*, World Scientific Publishing Co. Pte. Ltd., (2006)

ASKØY BRIDGE
Wind tunnel tests and analyses

Annex A

Theory

Contents in Annex A

A.1 Static load coefficients

The measurements carried out include drag C_D in the wind direction, lift C_L perpendicular to the wind direction and the overturning moment C_M. The mean drag, lift and moment load per unit length acting on bride decks is determined as:

Drag:
$$F_D(z) = q_m(z) h C_D \tag{A.1}$$

Lift:
$$F_L(z) = q_m(z) b C_L \tag{A.2}$$

Moment:
$$F_M(z) = q_m(z) b^2 C_M \tag{A.3}$$

where

b is the along-wind dimension of the structural part considered. Here the width of the bridge cross section ($b = 15.5$ m).

h is the cross-wind dimension of the structural part considered. Here the height of the bridge cross section ($h = 3.00$ m).

C_D, C_L, C_M are the drag, lift and moment coefficient, respectively.

$q_m(z)$ is the mean velocity pressure at height z defined by:

$$q_m(z) = \frac{1}{2} \rho_{air} U^2 \tag{A.4}$$

where ρ_{air} is the density of air and U is the time averaged air velocity.

A.2 Buffeting-induced vibrations

Buffeting tests have been carried out for the Askoy Bridge cross section. Any galloping response will also appear in the tests, however, no deviation is made between buffeting and galloping response. The tests both include buffeting response and investigation of critical flutter wind velocities.

In order to simulate critical flutter velocities correct, the frequency ratio of the torsional and vertical natural frequencies is important. The sensitivity of coupling of a vertical and torsional mode shape is dependent on the magnitude of the two natural frequencies and their internal frequency ratio. The higher natural frequencies and frequency ratio, the higher critical flutter velocities.

The sensitivity also highly depends on the mode coupling coefficient $C_\xi C_\alpha$, which is defined as:

$$C_\xi = \int^{deck} \xi(x)\alpha(x)\,dx \bigg/ \int^{deck} \xi^2(x)\,dx \qquad (A.5)$$

$$C_\alpha = \int^{deck} \xi(x)\alpha(x)\,dx \bigg/ \int^{deck} \alpha^2(x)\,dx \qquad (A.6)$$

where α and ξ are the torsional (along the bridge deck axis) and vertical mode shape. Similar vertical and torsional mode shapes, i.e. $C_\xi C_\alpha = 1$, indicates possible mode coupling. If $C_\xi C_\alpha = 0$ the mode shapes are not likely to couple. In the wind tunnel tests with section models both the vertical and torsional mode shapes have constant amplitude providing $C_\xi C_\alpha = 1$. Hence, the wind tunnel tests with section models will provide conservative results, when the investigated mode shapes have mode coupling coefficient $C_\xi C_\alpha < 1$, see [3].

A.3 Vortex-induced vibrations

When a body is located in a flow, vortices behind the body arises. These vortices occur periodically at each side of the body. In literature, the coincidence of eigenfrequency and vortex shedding frequency is described by a non-dimensional parameter referred to as the Strouhal number St. The Strouhal number is given as follows:

$$St = \frac{n_s h}{U_{crit}}$$

(A.7)

where

n_s is the vortex shedding frequency.

h is the vertical cross-wind dimension of the bridge deck.

U_{crit} is the critical air velocity.

The Strouhal number is dependent on the geometry of the body. For circular geometries the Strouhal number is close to 0.2 at low Reynolds numbers, while for rectangular geometries the Strouhal number varies depending on the ratio between the vertical cross-wind dimension and depth of the geometry. Figure A.1 shows the Strouhal number as a function of the cross section ratio for a rectangular geometry.
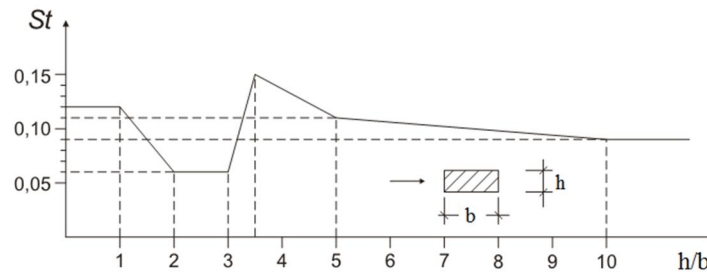
Figure A.1: Variation of Strouhal number for different rectangular cross sections with sharp edges [4].

If the vortices are formed with a frequency close to the body's eigenfrequency n_e, it could yield significant bending vibrations in a mode in the cross-wind direction. The air velocity in which these bending vibrations occur is known as the critical air velocity U_{crit} and is given as follows:

$$U_{crit} = \frac{1}{St} n_e h$$

(A.8)

In order to determine the vibrations of rectangular geometries, Eurocode 1 provides an approach depending on aerodynamic parameters and the physical properties of the structure. These are used in the Scruton number.

A.1.1 Scruton number

The Scruton number is in Eurocode 1 defined as follows:

$$Sc = \frac{2 \delta_s m_e}{\rho_{air} h^2}$$

(A.9)

where

δ_s is the structural damping expressed by the logarithmic decrement.

m_e is the effective mass per unit length.
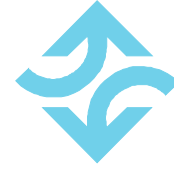
ρ_{air} is the air density.

The effective mass per unit length is given by:

$$m_e = \frac{M_g}{\int_0^h \xi^2(z)dz} \tag{A.10}$$

with

$\xi(z)$ being the mode shape.

M_g being the modal mass, which for a line-like structure with the span L can be determined in terms of the mode shape and the vibrating mass per unit length $m(z)$:

$$M_g = \int_0^L m(z)\xi^2(z)dz \tag{A.11}$$

What is worth noticing in Equation (A.9) is that the depth of the structure is left out, which could be due to the fact that Eurocode 1 also has to account for circular sections. However, a newly published paper by Svend Ole Hansen [2] contains a modified equation of the Scruton number under the assumption that the aerodynamic damping is proportional to the depth of the structure. Therefore, the equation given in [2] accounts for rectangular geometries by including the depth b. This equation is known as the general mass-damping parameter Sc_G and is given as follows:

$$Sc_G = \frac{2\delta_s m_e}{\rho h b} \tag{A.12}$$

The largest vortex shedding vibrations are most likely to occur at small values of the mass damping parameter.

The standard deviation of the vortex-induced structural deflection $\sigma_{y,max}$ at the point where the mode shape $\xi(z)$ has its largest deflection $\sigma_{y,max}$ is given by:

$$\frac{\sigma_{y,max}}{h} = \frac{1}{St^2} \frac{C_c}{\sqrt{\frac{Sc_G}{4\pi} - K_{aG}\left(1 - \left(\frac{\sigma_{y,max}}{a_L h}\right)^2\right)}} \sqrt{\frac{\rho_{air} h d}{m_e}} \sqrt{\frac{h}{l}} \tag{A.13}$$

where

C_c is an aerodynamic constant giving vibration amplitudes at high Sc_G.

K_{aG} is an aerodynamic damping factor.

a_L is the limit of the vibration of the structure with a very small damping.

l is the length of the bridge.

By solving Equation (A.13), the standard deviation of the structural deflection may be determined. The solution is given by:

$$\left(\frac{\sigma_{y,max}}{h}\right)^2 = c_1 + \sqrt{c_1^2 + c_2} \tag{A.14}$$

in which the constants c_1 and c_2 are equal to:

$$c_1 = \frac{a_L^2}{2}\left(1 - \frac{Sc_G}{4\pi K_{aG}}\right) \qquad\qquad c_2 = \frac{a_L^2}{K_{aG}}\frac{\rho_{air}d^2}{m_e}\frac{C_c^2}{St^4}\frac{h}{b} \qquad\qquad \text{(A.15)}$$

The maximum amplitude y_{max} is calculated by multiplying the standard deviation $\sigma_{y,max}$ with a peak factor k_p. At large amplitudes, the peak factor is equal to $\sqrt{2}$ while for intermediate amplitudes, the peak factor increases gradually with decreasing amplitude. The following simplified expression may be used to determine the peak factor:

$$k_p = \sqrt{2}\left(1 + 1.2\arctan\left(0.75\left(\frac{Sc_G}{4\pi K_{aG}}\right)\right)^4\right) \qquad\qquad \text{(A.16)}$$

ASKØY BRIDGE
Wind tunnel tests and analyses

Annex B

Static load coefficients, section model 1:50

Contents in Annex B

The figures and tables in this annex show the measured static load coefficients in the tests with section models of the Askøy bridge. Five configurations are investigated, see Table B.1. The tests have been carried out in turbulent flow with a turbulence intensity of approx. 13-15 %.

Table B.1: Tested configurations. All configurations have been tested in turbulent flow.

Config.	Bridge configuration	Angle [°]	Figure
1	Present bridge.	0, ±1.5, ±3, ±4, ±6, ±8, ±10	B.2
2a	One walkway upstream.	0, ±1.5, ±3, ±4, ±6, ±8, ±10	B.3
2c	One walkway upstream, guide vanes.	0, ±1.5, ±3, ±4, ±6, ±8, ±10	B.4
3	Present bridge, modified railings.	0, ±1.5, ±3, ±4, ±6, ±8, ±10	B.5
4	Two walkways.	0, ±1.5, ±3, ±4, ±6, ±8, ±10	B.6

The load components investigated are drag, lift, and moment. Drag is defined positive in the flow direction, lift is defined positive upwards and the moment is defined positive clockwise when the flow direction is from left to right. The load coefficients are given as a function of the incidence angle. Positive angles correspond to a rotation of the model where the upstream edge of the deck is raised, see Figure B.1. The incidence angle is to be understood as the sum of the mean wind's deviation from horizontal and the time average angular displacement, both positive for wind approach from underneath.

The static load coefficients are defined as:

Drag:
$$C_D = \frac{F_D}{q_m h l_m} \tag{B.1}$$

Lift:
$$C_L = \frac{F_L}{q_m b l_m} \tag{B.2}$$

Moment:
$$C_M = \frac{F_M}{q_m b^2 l_m} \tag{B.3}$$

with h being the cross-wind dimension of the bridge deck (3.00 m in full scale), b being the along-wind dimension of the bridge deck (15.5 m in full scale), l_m being the wind tunnel length of the bridge deck (the full scale length of the model deck section is 85.0 m) and q_m being the mean velocity pressure.
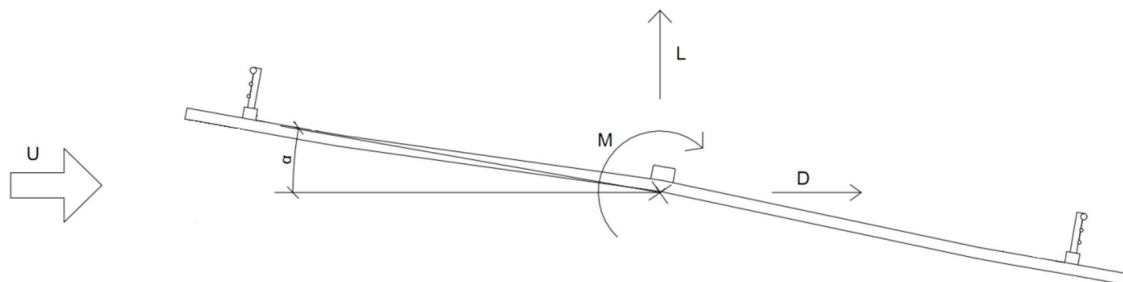
Figure B.1: Principle sketch of the definition of the incidence angle and wind loads acting on the bridge deck.

The main results are summarized in Table B.2.

Askøy Bridge
Wind tunnel tests and analyses
Annex B
Static load coefficients, section model 1:50
Revision 0, December 2014

Table B.2: Static load coefficients for measurements in static wind tunnel tests at an incidence angle of 0° (the numeric largest value in the range from -1.5° to 1.5° is shown - where both positive and negative values occur, both are shown). The slopes $dC_L/d\alpha$ and $dC_M/d\alpha$ are determined as the largest slope of a fitted second-degree polynomial in the interval -3° to 3°.

Config.	Drag, C_D	Lift, C_L	$dC_L/d\alpha$	Moment, C_M	$dC_M/d\alpha$
1	0.536	-0.329	5.632	-0.042/0.038	1.749
2a	0.699	-0.341	6.471	-0.025/0.137	3.154
2c	0.736	-0.440	4.981	-0.040/0.094	2.582
3	0.661	-0.461	5.464	-0.064/0.027	1.726
4	0.718	-0.412	6.669	-0.016/0.128	2.965

Askøy Bridge
Wind tunnel tests and analyses
Annex B
Static load coefficients, section model 1:50
Revision 0, December 2014

B.1 (1) PRESENT BRIDGE
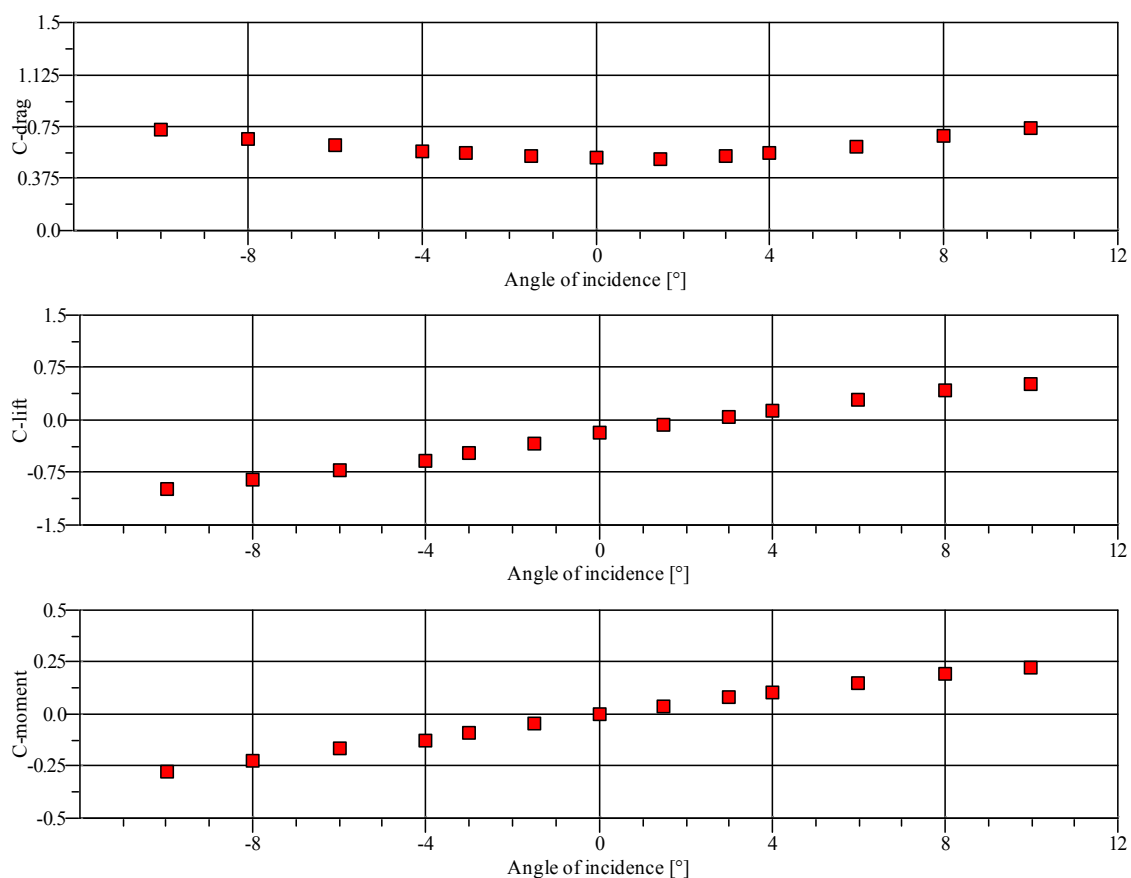
Angle of incidence [°	Static load coefficients [-]		
	Drag	Lift	Moment
-10.0	0.724	-0.984	-0.275
-8.0	0.662	-0.858	-0.225
-6.0	0.620	-0.708	-0.166
-4.0	0.572	-0.577	-0.124
-3.0	0.559	-0.477	-0.090
-1.5	0.536	-0.329	-0.042
0.0	0.524	-0.185	0.002
1.5	0.520	-0.068	0.038
3.0	0.539	0.053	0.079
4.0	0.560	0.132	0.104
6.0	0.606	0.288	0.153
8.0	0.679	0.425	0.197
10.0	0.738	0.516	0.223

Figure B.2: Static load coefficients for the configuration 1 (present bridge). Turbulent flow.

B.2 (2a) ONE WALKWAY UPSTREAM
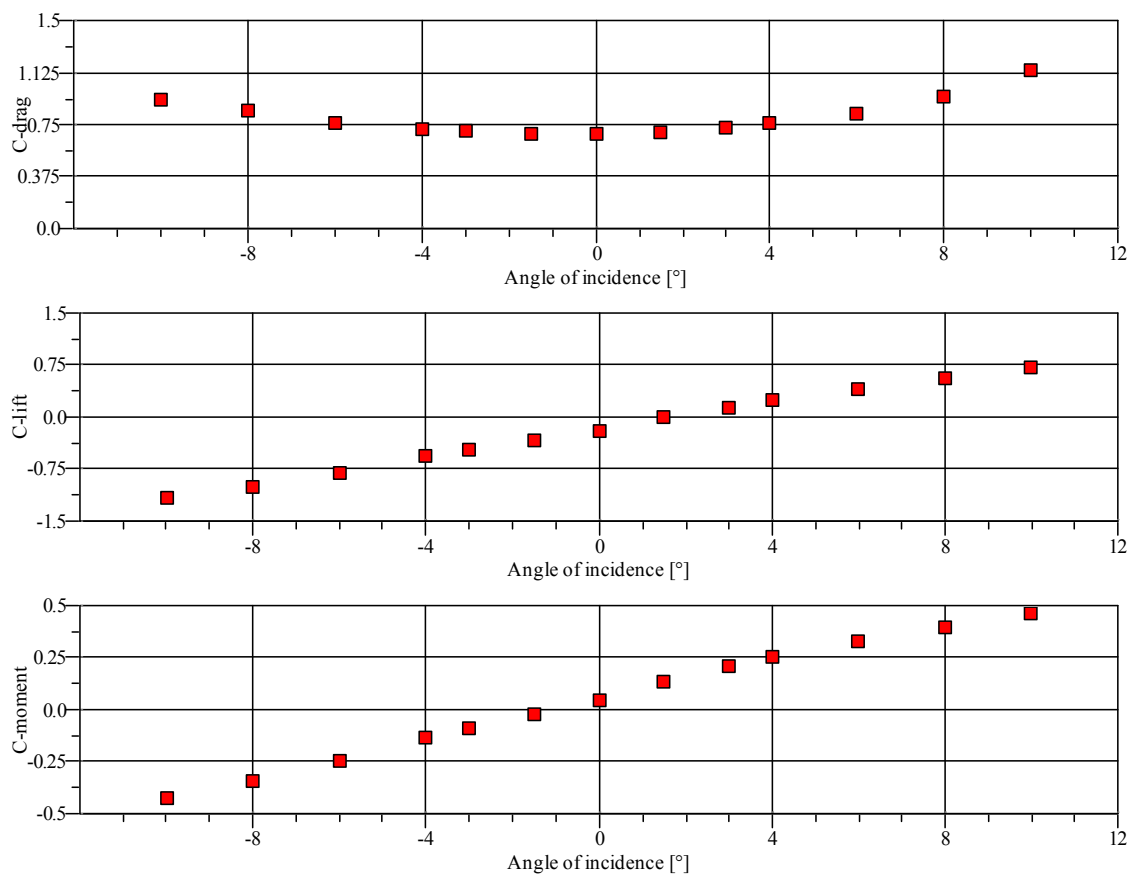
Angle of incidence [°	Static load coefficients [-]		
	Drag	Lift	Moment
-10.0	0.930	-1.165	-0.422
-8.0	0.852	-1.013	-0.344
-6.0	0.758	-0.796	-0.244
-4.0	0.718	-0.568	-0.132
-3.0	0.703	-0.480	-0.091
-1.5	0.684	-0.341	-0.025
0.0	0.680	-0.196	0.047
1.5	0.699	-0.001	0.137
3.0	0.726	0.142	0.210
4.0	0.758	0.240	0.255
6.0	0.825	0.410	0.330
8.0	0.952	0.568	0.396
10.0	1.139	0.723	0.463

Figure B.3: Static load coefficients for the configuration 2a (one walkway upstream). Turbulent flow.

B.3 (2c) ONE WALKWAY UPSTREAM, GUIDE VANES, VORTEX SPOILER
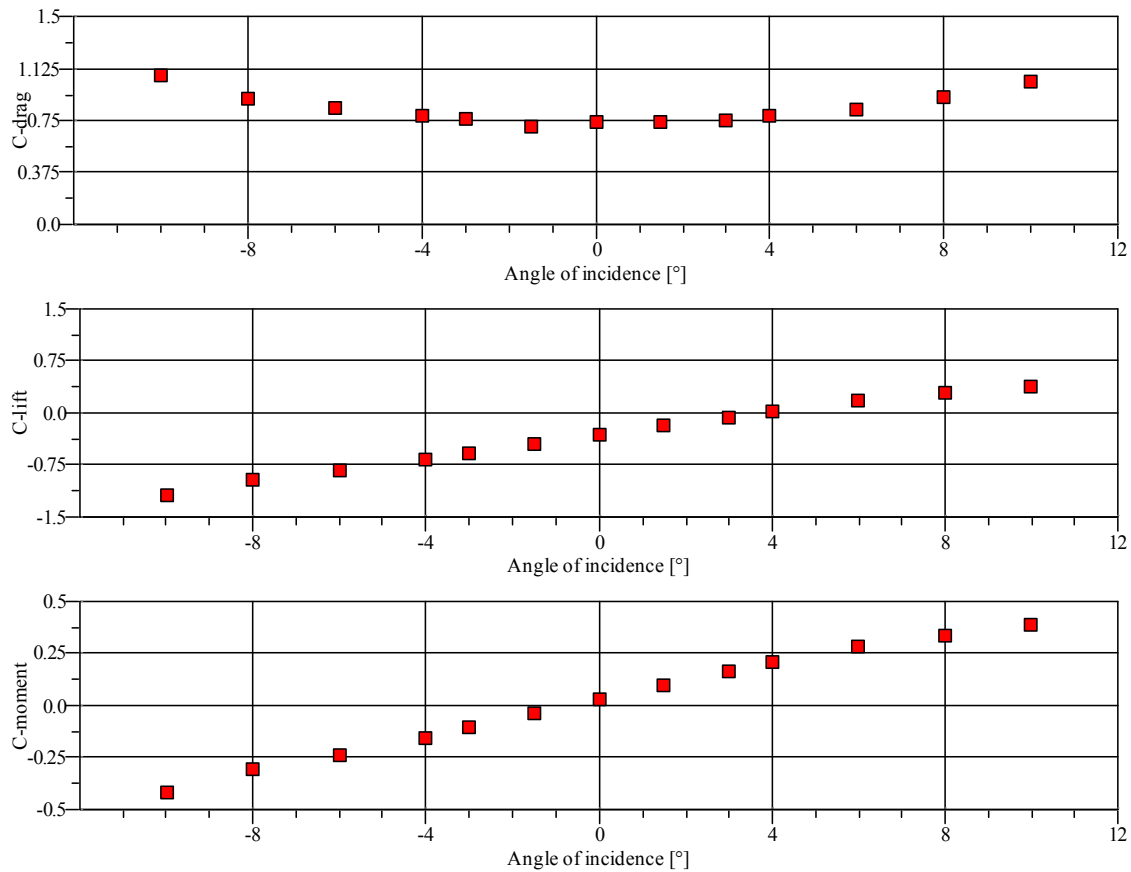
Angle of incidence [°	Static load coefficients [-]		
	Drag	Lift	Moment
-10.0	1.077	-1.176	-0.419
-8.0	0.912	-0.957	-0.303
-6.0	0.838	-0.834	-0.238
-4.0	0.784	-0.669	-0.154
-3.0	0.763	-0.575	-0.106
-1.5	0.708	-0.440	-0.040
0.0	0.736	-0.315	0.031
1.5	0.736	-0.188	0.093
3.0	0.753	-0.060	0.162
4.0	0.780	0.024	0.207
6.0	0.834	0.179	0.284
8.0	0.914	0.290	0.339
10.0	1.024	0.380	0.390

Figure B.4: Static load coefficients for the configuration 2c (one walkway upstream, guide vanes, vortex spoiler). Turbulent flow.

B.4 (3) PRESENT BRIDGE, MODIFIED RAILINGS
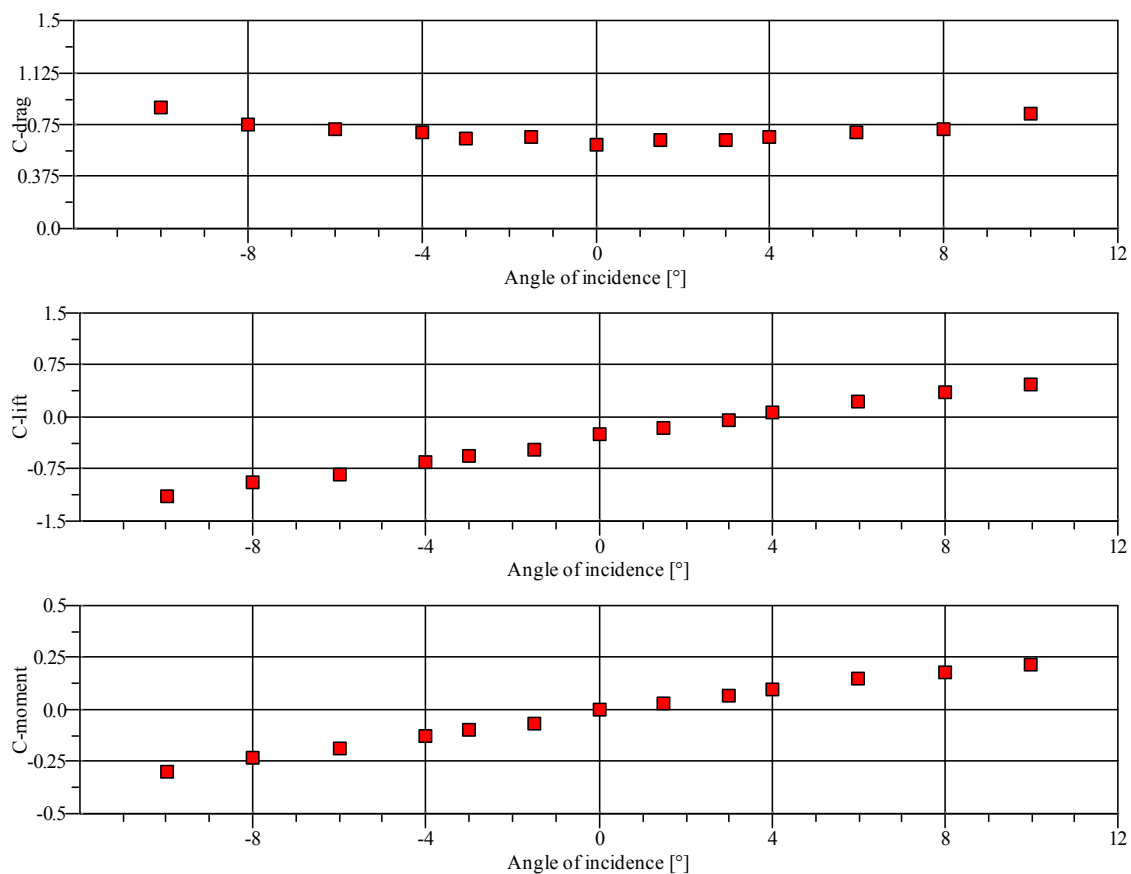
Angle of incidence [°	Static load coefficients [-]		
	Drag	Lift	Moment
-10.0	0.868	-1.135	-0.300
-8.0	0.752	-0.939	-0.231
-6.0	0.715	-0.817	-0.186
-4.0	0.694	-0.658	-0.126
-3.0	0.652	-0.557	-0.096
-1.5	0.661	-0.461	-0.064
0.0	0.605	-0.254	-0.001
1.5	0.635	-0.166	0.027
3.0	0.633	-0.035	0.067
4.0	0.656	0.058	0.097
6.0	0.694	0.232	0.152
8.0	0.720	0.351	0.181
10.0	0.832	0.481	0.219

Figure B.5: Static load coefficients for the configuration 3 (present bridge, modified railings). Turbulent flow.

B.5   (4) TWO WALKWAYS
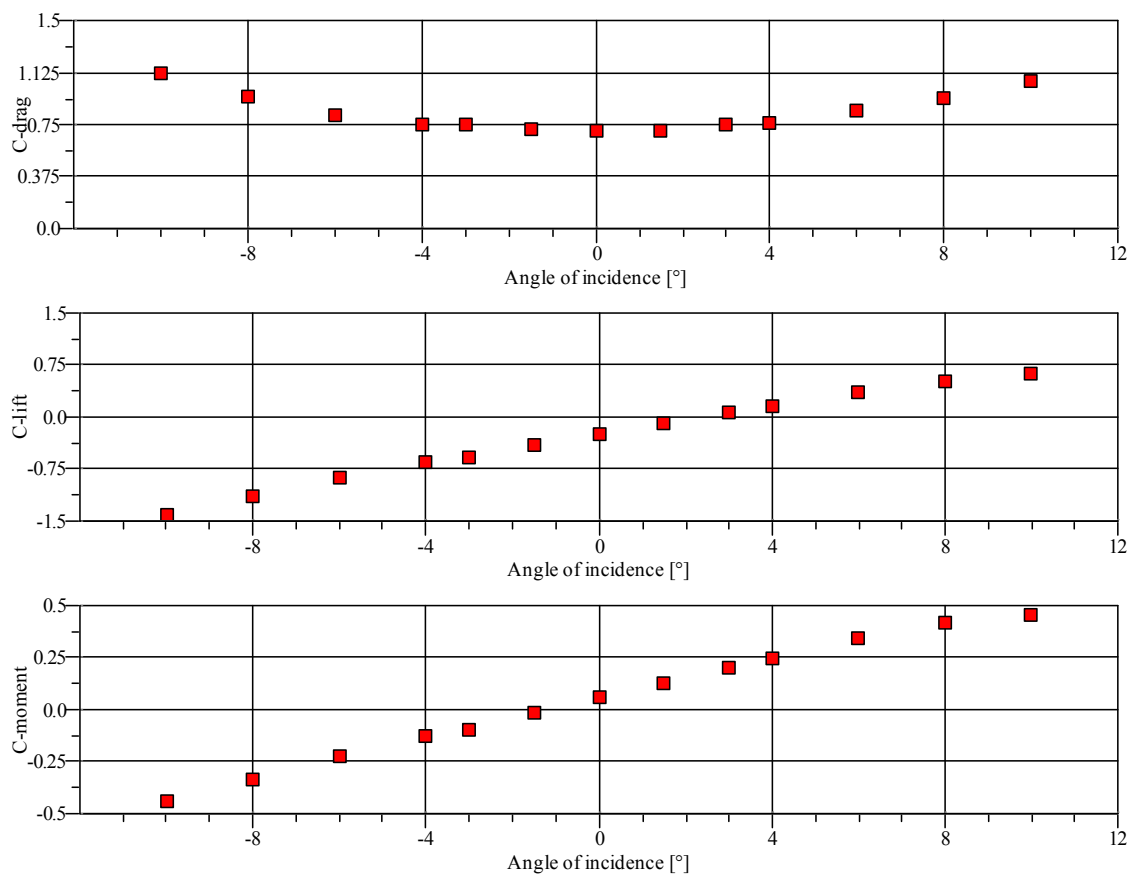
Angle of incidence [°	Static load coefficients [-]		
	Drag	Lift	Moment
-10.0	1.119	-1.401	-0.441
-8.0	0.951	-1.148	-0.336
-6.0	0.814	-0.875	-0.223
-4.0	0.753	-0.658	-0.126
-3.0	0.748	-0.588	-0.095
-1.5	0.718	-0.412	-0.016
0.0	0.704	-0.239	0.061
1.5	0.705	-0.095	0.128
3.0	0.752	0.061	0.203
4.0	0.759	0.150	0.243
6.0	0.856	0.366	0.345
8.0	0.942	0.519	0.415
10.0	1.066	0.628	0.457

Figure B.6: Static load coefficients for the configuration 4 (two walkways). Turbulent flow.

ASKØY BRIDGE
Wind tunnel tests and analyses

Annex C

Buffeting-induced vibrations, section model 1:50

Contents in Annex C

The figures and tables in this annex show the response measured in the buffeting tests with a section model of the Askøy bridge deck. All figures and tables show the response for the frequency ratio based on a symmetric vertical and torsional mode given by Statens vegvesen.

The theory behind this annex may be seen in Annex A. Six configurations are investigated, see Table C.1. All the tests have been carried out in turbulent flow with a turbulence intensity in the wind direction of approx. 13-15% and at an incidence angle of 0°. Note that the frequency ratio for configuration 1 and 3 are lower than the full scale frequency ratio. This means that the results will be conservative.

Table C.1: Investigated configurations. All measurements are conducted in turbulent flow.

Config.	Bridge configuration	Freq. heave n_H [Hz]		Freq. torsion n_T [Hz]		Freq. ratio n_T/n_H [-]		Figure
		MS	FS	MS	FS	MS	FS	
1	Present bridge.	1.25	0.19	3.10	0.58	2.49	3.11	C.1
2a	One walkway upstream.	1.23	0.18	3.09	0.47	2.51	2.59	C.2
2b	One walkway downstream.	1.27	0.18	3.41	0.47	2.68	2.59	C.3
2c	One walkway upstream, guide vanes.	1.25	0.18	3.28	0.47	2.62	2.59	C.4
3	Present bridge, modified railings.	1.30	0.19	3.21	0.58	2.48	3.11	C.5
4	Two walkways.	1.20	0.18	3.02	0.47	2.52	2.59	C.6

The buffeting responses are measured for a period corresponding to approx. 13 minutes in full scale.

The vertical displacements of the models are shown normalised with the height of the bridge deck (3.00 m in full scale). Positive vertical displacement has been defined "upwards" and positive rotation of the model "with the windward side up". The response is given as a function of normalised wind velocity.

The wind velocity is normalised with the width of the bridge deck (15.5 m in full scale) and the natural frequencies in still air. In order to get full scale wind velocities, the normalised wind velocity is multiplied with the full scale frequency and the full scale bridge deck height.

For heave, full scale accelerations of the bridge deck may be determined by:

$$a_{\text{FS},H} = r \cdot \left(2 \cdot \pi \cdot n_{H,\text{FS}}\right)^2$$

For torsion, full scale accelerations at the outer edge of the bridge deck may be determined by:

$$a_{\text{FS},T} = \sin(\Phi) \cdot b_{\text{FS}}/2 \cdot \left(2 \cdot \pi \cdot n_{T,\text{FS}}\right)^2$$

The following symbols have been used:
b - Width of bridge deck corresponding to 15.5 m in full scale.
h - Height of bridge deck corresponding to 3.00 m in full scale.
m_e - Mass per unit length.
n - Natural frequency in still air.
r - Vertical displacement.

Askøy bridge
Wind tunnel tests and analyses
Annex C
Buffeting-induced vibrations, section model 1:50
Revision 0, January 2015

FS - Full scale.

H - Heave.

MS - Model scale.

T - Torsion.

U - Mean wind velocity.

Φ - Torsional displacement.

The mass and mass moment of inertia of the models investigated are shown in Table C.2 and Table C.3, respectively.

Table C.2: Masses of wind tunnel model compared to full scale structure.

Config.	$m_{e,FS}$ [kg/m]	$m_{e,MS,target}$ [kg/m]	$m_{e,MS}$ [kg/m]	Deviation [%]
1	9287	3.72	4.04	8.63
2a	10445	4.18	4.12	1.43
2b	10445	4.18	3.88	7.17
2c	10445	4.18	3.99	4.41
3	9287	3.72	3.69	0.56
4	10445	4.18	4.13	1.14

Table C.3: Mass moment of inertia of wind tunnel model compared to full scale structure.

Config.	$I_{e,FS}$ [kgm²/m]	$I_{e,MS,target}$ [kgm²/m]	$I_{e,MS}$ [kgm²/m]	Deviation [%]
1	242752	0.039	0.041	4.72
2a	350052	0.056	0.057	1.73
2b	350052	0.056	0.055	1.58
2c	350052	0.056	0.060	6.25
3	242752	0.039	0.038	2.65
4	350052	0.056	0.060	6.47

The normalised data represents full scale values for a structure, where modal mass, mode shapes, damping ratio, etc. correspond to model conditions.
The model results represent conditions with a modal coupling coefficient of 1.

The dynamic properties and measured displacements of the tested sections may be viewed in Table C.4 for heave and torsion. For the present bridge with and without the modified railings, flutter is not observed up to approx. 70 m/s. Flutter is, however, observed to occur near 60 m/s when a walkway is positioned upstream. Flutter does not occur up to approx. 70 m/s when the walkway is positioned downstream. A research of wind statistics on site should therefore be conducted to enlighten the probability of high wind velocities for the wind direction with upstream walkway. Furthermore, flutter has been observed near 60 m/s for the bridge section with two walkways.

Table C.4: Dynamic properties and measured displacements of the tested sections for heave and torsion at approx. 60 m/s. All measurements have been conducted in turbulent flow. [*] denotes that flutter occurs near 60 m/s.

Config.	Damping		Max. displacement	
	δ_H [% LD]	δ_T [% LD]	r/h [-]	Φ [°]
1	2.1	0.6	0.62	4.53
2a[*]	2.7	1.3	0.37	6.38
2b	1.9	0.9	0.51	3.76
2c[*]	2.5	0.7	0.19	7.62
3	2.1	0.6	0.35	3.69
4[*]	3.8	1.3	0.16	1.97

C.1. (1) PRESENT BRIDGE
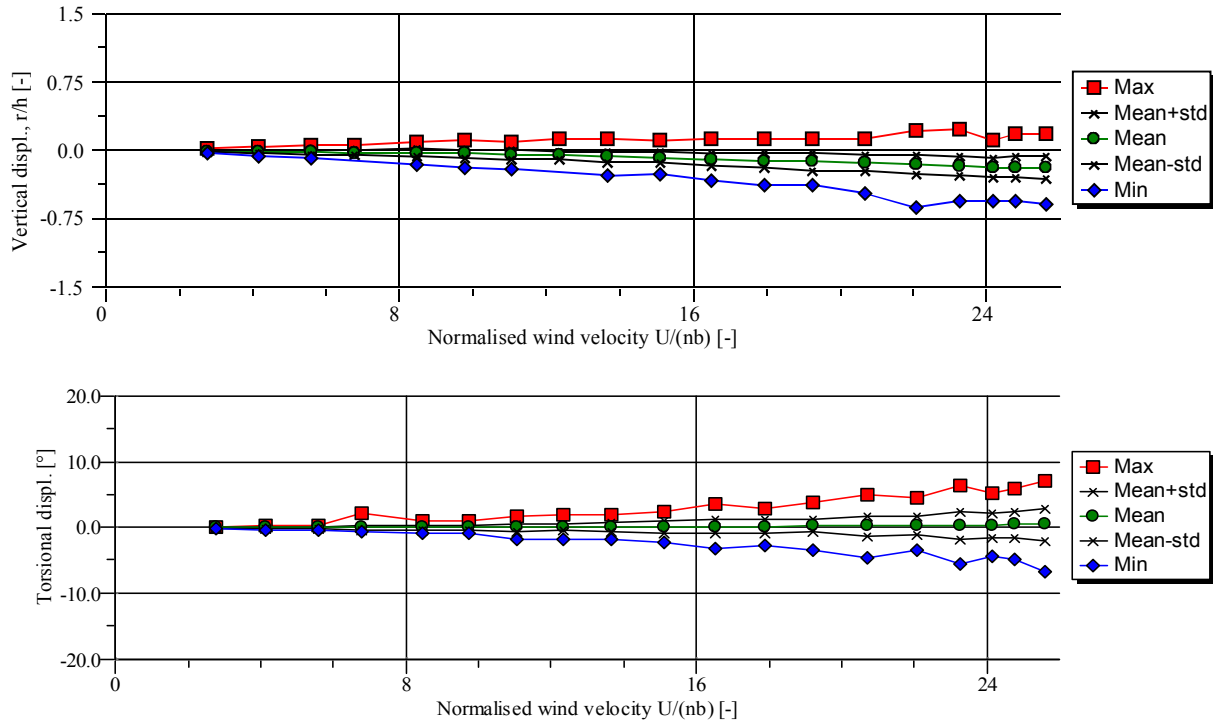
$U/(n_H b)$ [-]	Vertical displacement, r/h [-]				Torsional displacement, ϕ [°]			
	Mean	Std	Max	Min	Mean	Std	Max	Min
2.76	-0.0035	0.0068	0.0214	-0.0310	0.0045	0.0246	0.1000	-0.0907
4.15	-0.0074	0.0161	0.0460	-0.0697	0.0121	0.1214	0.2951	-0.2969
5.58	-0.0124	0.0248	0.0575	-0.0839	0.0205	0.1220	0.3515	-0.3086
6.77	-0.0189	0.0280	0.0660	-	0.0324	0.3089	2.1894	-0.6753
8.46	-0.0253	0.0439	0.0997	-0.1471	0.0488	0.4080	0.9896	-0.8848
9.75	-0.0330	0.0467	0.1157	-0.1766	0.0656	0.3439	1.0964	-0.9236
11.04	-0.0418	0.0541	0.0979	-0.1948	0.0833	0.5891	1.8128	-1.7085
12.32	-0.0519	0.0496	0.1271	-	0.1073	0.4794	1.9250	-1.7359
13.64	-0.0660	0.0635	0.1302	-0.2643	0.1248	0.6369	1.9788	-1.6817
15.10	-0.0764	0.0631	0.1076	-0.2528	0.1581	0.9021	2.5347	-2.3176
16.51	-0.0938	0.0743	0.1366	-0.3326	0.1837	1.0366	3.5864	-3.1833
17.91	-0.1065	0.0830	0.1345	-0.3833	0.2328	0.9949	2.9476	-2.6708
19.24	-0.1212	0.0899	0.1236	-0.3845	0.2591	0.9292	3.8917	-3.4027
20.70	-0.1322	0.0955	0.1248	-0.4722	0.3073	1.5536	4.9336	-4.5215
22.07	-0.1500	0.0983	0.2280	-0.6225	0.3561	1.3923	4.5338	-3.4142
23.27	-0.1663	0.1114	0.2452	-0.5521	0.3982	2.1390	6.3425	-5.5784
24.15	-0.1798	0.1073	0.1188	-0.5552	0.4414	1.8509	5.3566	-4.2614
24.76	-0.1786	0.1126	0.1788	-0.5443	0.4923	1.9014	5.9431	-4.8563
25.60	-0.1851	0.1178	0.1897	-0.5943	0.5311	2.4506	7.1512	-6.5896

Figure C.1: Buffeting-induced vibrations of Askøy Bridge configuration 1 (present bridge) at incidence angle 0°. The logarithmic damping decrement is 2.1% for heave and 0.6% for torsion. The frequency ratio is 2.49. n is the vertical frequency in still air.

C.2. (2a) ONE WALKWAY UPSTREAM
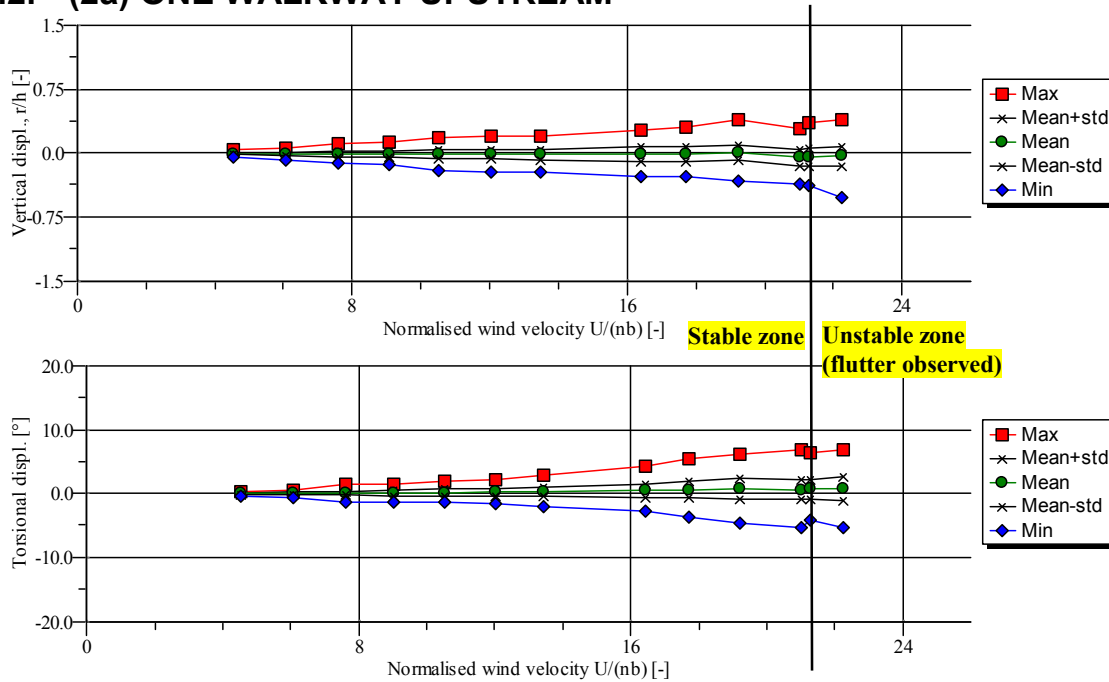
$U/(n_H b)$ [-]	Vertical displacement, r/h [-]				Torsional displacement, ϕ [°]			
	Mean	Std	Max	Min	Mean	Std	Max	Min
4.53	-0.0032	0.0131	0.0462	-0.0525	0.0246	0.0862	0.3109	-0.2486
6.07	-0.0051	0.0195	0.0628	-0.0706	0.0498	0.1863	0.6622	-0.5507
7.61	-0.0066	0.0312	0.1058	-0.1184	0.0867	0.3022	1.4486	-1.2076
9.05	-0.0086	0.0387	0.1241	-0.1371	0.1298	0.3956	1.4480	-1.2456
10.51	-0.0096	0.0556	0.1823	-0.2086	0.1920	0.5441	1.8775	-1.3521
12.04	-0.0112	0.0505	0.1980	-0.2177	0.2556	0.5534	2.1365	-1.5462
13.46	-0.0126	0.0605	0.1962	-0.2247	0.3402	0.6955	3.0334	-1.9569
16.42	-0.0083	0.0860	0.2681	-0.2765	0.5614	1.0315	4.2145	-2.6939
17.70	-0.0023	0.0870	0.3057	-0.2798	0.6943	1.3691	5.5291	-3.6195
19.23	0.0080	0.0925	0.3879	-0.3164	0.8508	1.6228	6.2340	-4.6699
21.03	-0.0500	0.1006	0.2811	-0.3684	0.6523	1.5178	6.9034	-5.1545
21.27	-0.0436	0.1091	0.3657	-0.3691	0.7402	1.5667	6.3764	-4.1582
22.27	-0.0328	0.1105	0.3922	-0.5178	0.8478	1.8918	6.9233	-5.1944

Figure C.2: Buffeting-induced vibrations of Askøy Bridge configuration 2a (one walkway upstream) at incidence angle 0°. The logarithmic damping decrement is 2.7% for heave and 1.3% for torsion. The frequency ratio is 2.51. n is the vertical frequency in still air.

C.3. (2b) ONE WALKWAY DOWNSTREAM
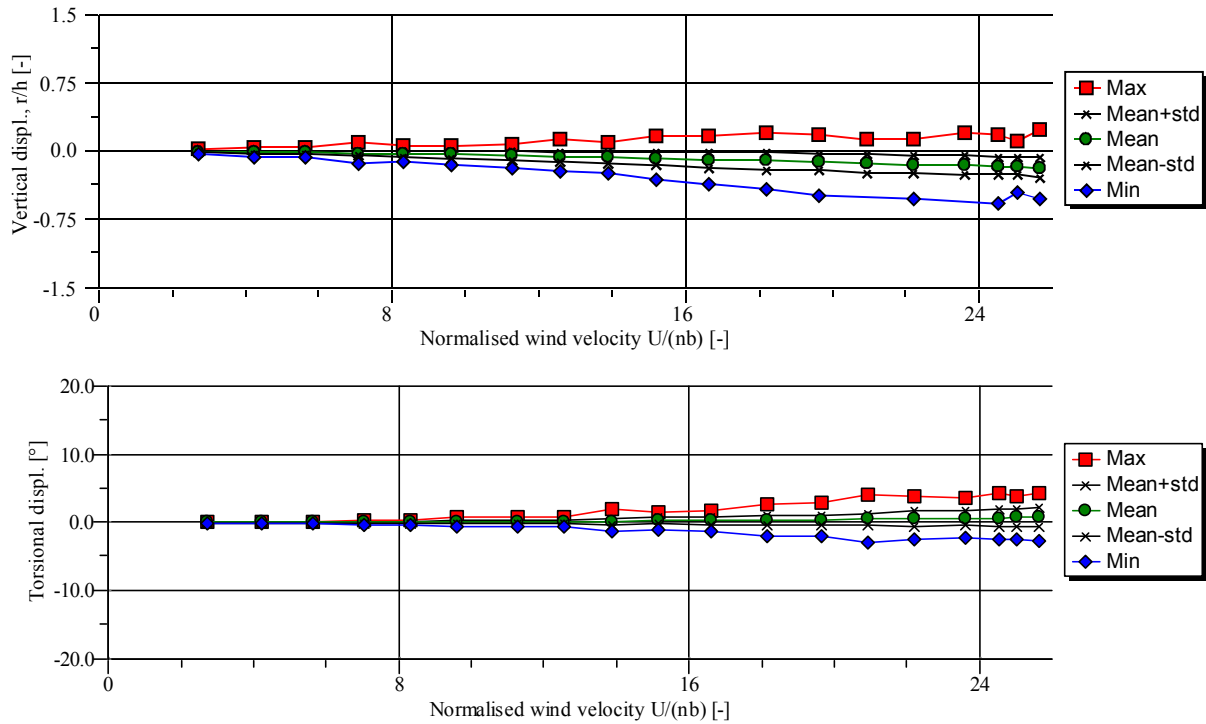
$U/(n_H b)$ [-]	Vertical displacement, r/h [-]				Torsional displacement, ϕ [°]			
	Mean	Std	Max	Min	Mean	Std	Max	Min
2.71	-0.0035	0.0080	0.0239	-0.0290	0.0069	0.0175	0.0675	-0.0676
4.21	-0.0073	0.0105	0.0517	-0.0654	0.0153	0.0277	0.1414	-0.0921
5.63	-0.0118	0.0171	0.0436	-0.0671	0.0292	0.0314	0.1627	-0.0773
7.07	-0.0180	0.0313	0.0928	-0.1230	0.0459	0.0742	0.3445	-0.2343
8.31	-0.0264	0.0315	0.0589	-0.1093	0.0677	0.1033	0.4358	-0.2740
9.62	-0.0343	0.0381	0.0605	-0.1479	0.0909	0.1594	0.7173	-0.4734
11.26	-0.0451	0.0468	0.0835	-0.1840	0.1195	0.2185	0.8208	-0.5424
12.55	-0.0547	0.0533	0.1302	-0.2247	0.1524	0.2411	0.8490	-0.5095
13.87	-0.0676	0.0569	0.0915	-0.2335	0.1964	0.4327	1.9401	-1.2881
15.17	-0.0780	0.0724	0.1634	-0.3111	0.2429	0.4735	1.5416	-1.0206
16.63	-0.0956	0.0807	0.1663	-	0.2934	0.5281	1.7469	-1.3111
18.17	-0.0999	0.0938	0.1966	-0.4120	0.3413	0.6167	2.6133	-1.9041
19.65	-0.1164	0.0874	0.1916	-0.4797	0.4063	0.7116	2.9328	-1.9559
20.92	-0.1291	0.1057	0.1262	-2.9803	0.4716	0.9264	4.1292	-2.9970
22.22	-0.1415	0.0896	0.1347	-0.5103	0.5385	1.1035	3.7604	-2.3597
23.62	-0.1494	0.1072	0.2009	-	0.6584	1.0172	3.6906	-2.2840
24.53	-0.1583	0.0959	0.1807	-0.5681	0.6888	1.2119	4.2442	-2.5268
25.03	-0.1655	0.0963	0.1106	-0.4434	0.7434	1.2521	3.7575	-2.3973
25.67	-0.1761	0.1076	0.2433	-0.5209	0.7657	1.4091	4.3860	-2.7597

Figure C.3: Buffeting-induced vibrations of Askøy Bridge configuration 2b (one walkway downstream) at incidence angle 0°. The logarithmic damping decrement is 1.9% for heave and 0.9% for torsion. The frequency ratio is 2.68. n is the vertical frequency in still air.

C.4. (2c) ONE WALKWAY UPSTREAM, GUIDE VANES
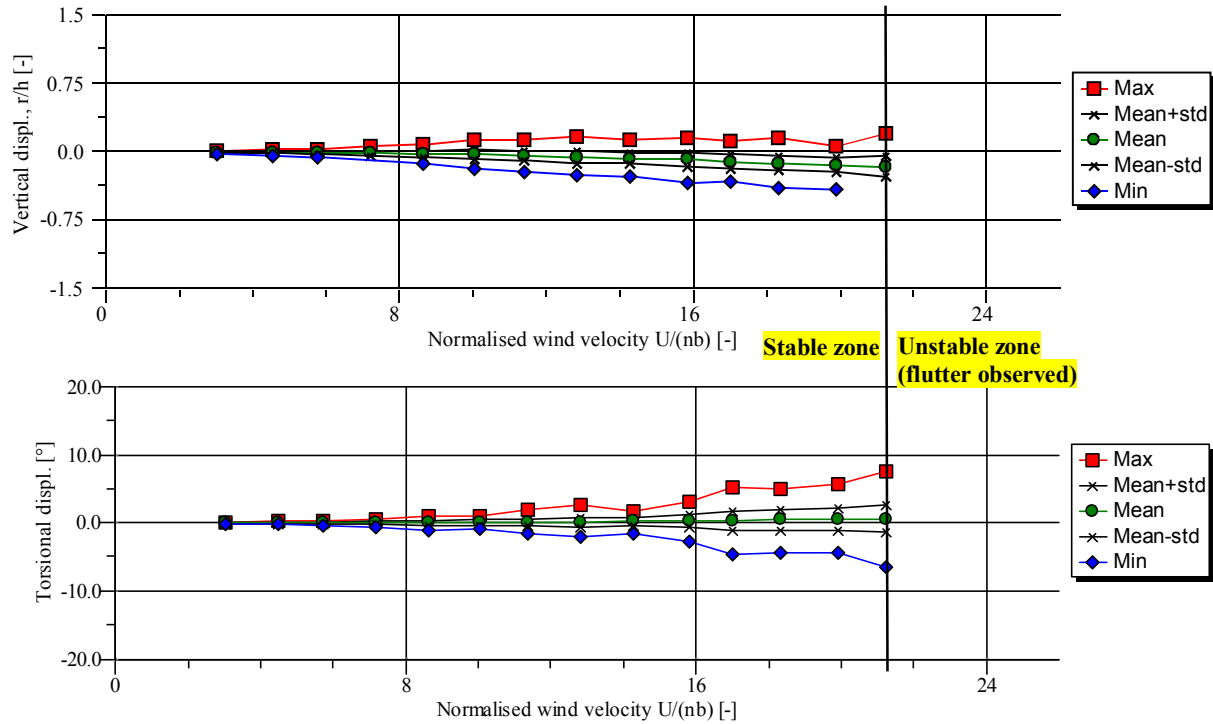
$U/(n_Hb)$ [-]	Vertical displacement, r/h [-]				Torsional displacement, ϕ [°]			
	Mean	Std	Max	Min	Mean	Std	Max	Min
3.02	-0.0018	0.0057	0.0165	-0.0243	0.0137	0.0308	0.1161	-0.0903
4.52	-0.0048	0.0088	0.0250	-0.0369	0.0238	0.0746	0.2424	-0.1887
5.75	-0.0097	0.0134	0.0343	-0.0528	0.0379	0.1118	0.4140	-0.2857
7.19	-0.0156	0.0302	0.0620	-0.6240	0.0629	0.2355	0.6911	-0.6137
8.64	-0.0232	0.0315	0.0738	-	0.0883	0.3509	1.1596	-0.9611
10.05	-0.0326	0.0510	0.1261	-0.1848	0.1199	0.3776	1.0483	-0.8957
11.38	-0.0449	0.0503	0.1287	-0.2189	0.1555	0.4951	1.8896	-1.6312
12.84	-0.0592	0.0640	0.1676	-0.2570	0.1974	0.7262	2.6422	-1.8737
14.28	-0.0744	0.0657	0.1383	-0.2805	0.2442	0.6349	1.8532	-1.4540
15.83	-0.0862	0.0795	0.1471	-0.3507	0.3219	0.9598	3.2348	-2.7264
17.03	-0.1094	0.0777	0.1165	-0.3221	0.3915	1.4619	5.3769	-4.6059
18.32	-0.1273	0.0809	0.1463	-0.3933	0.4831	1.5822	5.1368	-4.3495
19.91	-0.1458	0.0786	0.0541	-0.4082	0.5874	1.5809	5.6419	-4.2910
21.23	-0.1631	0.1128	0.1939	-	0.6902	1.9801	7.6234	-6.4788

Figure C.4: Buffeting-induced vibrations of Askøy Bridge configuration 2c (one walkway upstream, guide vanes) at incidence angle 0°. The logarithmic damping decrement is 2.5% for heave and 0.7% for torsion. The frequency ratio is 2.62. n is the vertical frequency in still air.

C.5. (3) PRESENT BRIDGE, MODIFIED RAILINGS
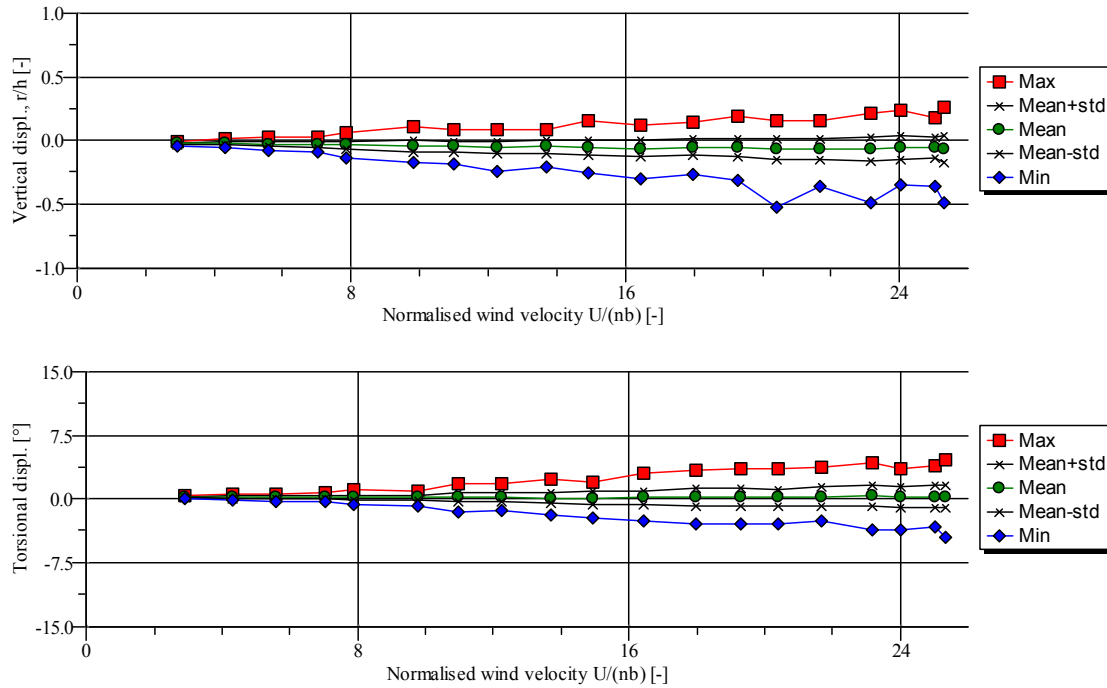
$U/(n_Hb)$ [-]	Vertical displacement, r/h [-]				Torsional displacement, ϕ [°]			
	Mean	Std	Max	Min	Mean	Std	Max	Min
2.92	-0.0202	0.0052	-0.0047	-0.0362	0.2577	0.0395	0.4052	0.0886
4.32	-0.0211	0.0115	0.0128	-0.0541	0.2388	0.1368	0.6035	-0.1183
5.60	-0.0244	0.0143	0.0246	-0.0748	0.2315	0.1701	0.6869	-0.2723
7.04	-0.0279	0.0220	0.0338	-0.0934	0.2263	0.1488	0.7378	-0.2417
7.87	-0.0310	0.0305	0.0683	-0.1326	0.2243	0.2299	1.1193	-0.6856
9.81	-0.0373	0.0453	0.1134	-0.1718	0.2294	0.2900	1.0166	-0.7835
10.99	-0.0427	0.0419	0.0894	-0.1777	0.2448	0.5407	1.7772	-1.4246
12.27	-0.0492	0.0472	0.0930	-0.2425	0.2769	0.4757	1.7635	-1.3213
13.70	-0.0449	0.0489	0.0907	-0.2079	0.1628	0.5557	2.4433	-1.8138
14.92	-0.0552	0.0558	0.1523	-0.2527	0.1618	0.7297	2.0472	-2.2542
16.43	-0.0594	0.0645	0.1224	-0.3022	0.1917	0.8105	3.0066	-2.6159
17.98	-0.0494	0.0668	0.1518	-0.2644	0.1970	1.0719	3.4303	-2.8655
19.28	-0.0572	0.0703	0.1894	-0.3110	0.2245	1.0036	3.6293	-2.8408
20.40	-0.0638	0.0804	0.1608	-0.5210	0.2211	0.9636	3.6706	-2.8890
21.69	-0.0645	0.0801	0.1539	-0.3531	0.3043	1.1245	3.6870	-2.5010
23.17	-0.0640	0.0914	0.2207	-0.4808	0.3605	1.2348	4.2143	-3.5436
24.02	-0.0573	0.0928	0.2451	-0.3455	0.2420	1.2718	3.6057	-3.6104
25.03	-0.0529	0.0848	0.1768	-0.3569	0.3176	1.3130	3.9453	-3.2478
25.32	-0.0627	0.1060	0.2635	-0.4799	0.3454	1.2747	4.7135	-4.4387

Figure C.5: Buffeting-induced vibrations of Askøy Bridge configuration 3 (present bridge, modified railings) at incidence angle 0°. The logarithmic damping decrement is 2.1% for heave and 0.6% for torsion. The frequency ratio is 2.48. n is the vertical frequency in still air.

C.6. (4) TWO WALKWAYS
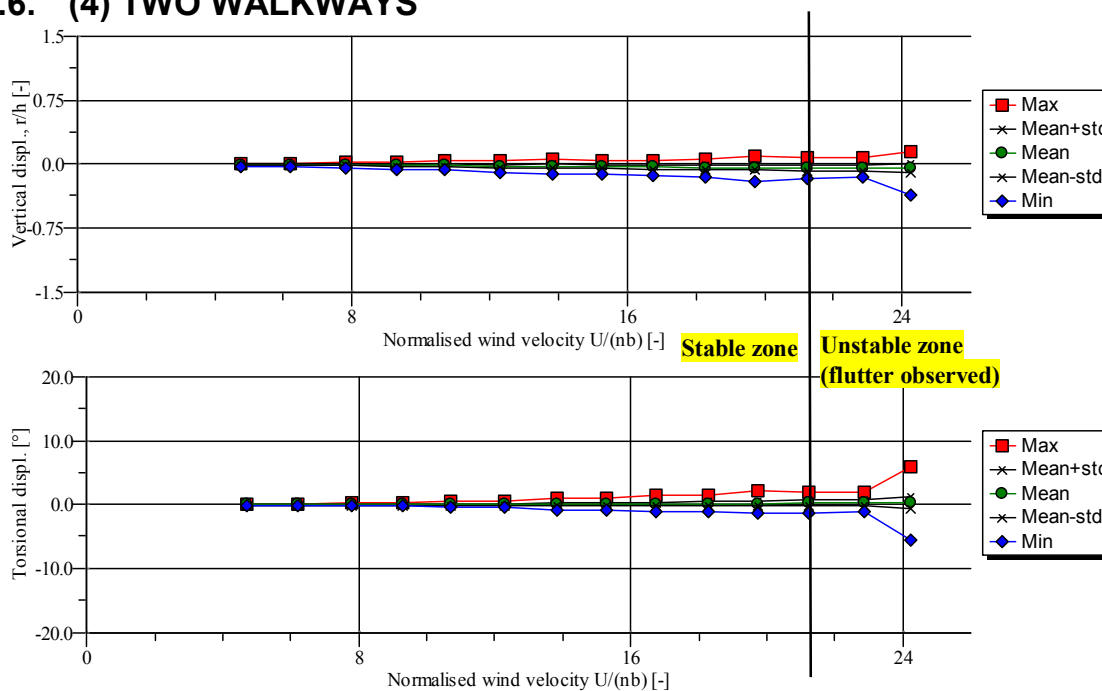
$U/(n_Hb)$ [-]	Vertical displacement, r/h [-]				Torsional displacement, ϕ [°]			
	Mean	Std	Max	Min	Mean	Std	Max	Min
4.73	-0.0029	0.0049	0.0129	-0.0179	0.0077	0.0198	0.0790	-0.0725
6.21	-0.0050	0.0071	0.0155	-0.0266	0.0143	0.0310	0.1291	-0.0995
7.82	-0.0077	0.0083	0.0193	-0.0424	0.0243	0.0563	0.2409	-0.1687
9.28	-0.0109	0.0109	0.0339	-0.0573	0.0365	0.0770	0.2914	-0.2106
10.71	-0.0146	0.0159	0.0415	-0.0697	0.0507	0.1258	0.5439	-0.4571
12.30	-0.0190	0.0184	0.0436	-0.0968	0.0659	0.1450	0.6570	-0.4515
13.84	-0.0225	0.0227	0.0615	-0.1105	0.0886	0.2040	0.9500	-0.7371
15.28	-0.0278	0.0236	0.0522	-0.1222	0.1103	0.2236	1.0375	-0.7248
16.76	-0.0320	0.0254	0.0483	-0.1289	0.1410	0.3042	1.4119	-1.0638
18.27	-0.0360	0.0267	0.0619	-0.1475	0.1760	0.3361	1.4726	-0.9812
19.73	-0.0398	0.0303	0.0951	-0.1950	0.2155	0.4198	2.1106	-1.3805
21.23	-0.0421	0.0333	0.0778	-0.1637	0.2679	0.4790	1.9695	-1.4001
22.85	-0.0421	0.0345	0.0833	-0.1512	0.3323	0.5072	1.9743	-1.1301
24.24	-0.0456	0.0519	0.1528	-0.3595	0.3945	0.9926	6.0177	-5.5856

Figure C.6: Buffeting-induced vibrations of Askøy Bridge configuration 4 (two walkways) at incidence angle 0°. The logarithmic damping decrement is 3.8% for heave and 1.3% for torsion. The frequency ratio is 2.52. n is the vertical frequency in still air.

ASKOY BRIDGE
Wind tunnel tests and analyses

Annex D

Vortex-induced vibrations, section model 1:50

Contents in Annex D

The figures and tables in this annex show the response measured in the vortex shedding tests with a section model of the Askøy Bridge. The theory behind this annex can be seen in Annex A. Five configurations are investigated, see Table D.1. All the tests have been carried out in low turbulent flow.

Table D.1: Investigated configurations. All tests have been carried out in low turbulent flow.

Config.	Bridge configuration	Figure
1	Present bridge.	D.1-D.5
2a	One walkway upstream.	D.6-D.10
2b	One walkway downstream.	D.11-D.12
2c	One walkway upstream, guide vanes.	D.13
2d	One walkway upstream, guide vanes, vortex spoiler.	D.14-D.15
3	Present bridge, modified railings.	D.16-D.21
4	Two walkways.	D.22-D.23

The displacements of the models are shown normalised by the height of the bridge deck, h_{FS} = 3.00 m. Positive vertical displacement has been defined "upwards" and positive rotation of the model "with the windward side up". The response is given as a function of normalised wind velocity.

The air velocity is normalised by the height of the bridge deck h_{FS} = 3.00 m and the vertical frequency in still air. In order to get full scale wind velocities, the normalised wind velocity is multiplied by the full scale frequency and height of the bridge deck.

The following symbols are used:

a - Max accelerations.
b - Along-wind width of bridge deck.
h - Height of bridge deck.
m_e - Mass per unit length.
n_H - Vertical frequency.
n_T - Torsional frequency.
r - Vertical displacement.
FS - Full-scale.
H - Heave.
MS - Model scale.
T - Torsion.
U - Mean wind velocity.
U_{crit} - Resonance wind velocity.
Φ - Torsional displacement.

The mass and mass moment of inertia of the section models investigated are shown in Table D.2 and Table D.3, respectively.

Table D.2: Masses of wind tunnel model compared to full-scale structure for heave.

Config.	$m_{e,FS}$ [kg/m]	$m_{e,MS,target}$ [kg/m]	$m_{e,MS}$ [kg/m]	Deviation [%]
1	9287	3.72	3.63-3.78	2.29-1.60
2a	10445	4.18	3.81-4.21	8.80-0.71
2b	10445	4.18	3.98	4.76
2c	10445	4.18	4.05	2.99
2d	10445	4.18	4.05	2.99
3	9287	3.72	3.64-3.78	2.21-1.68
4	10445	4.18	3.93	6.01

Table D.3: Mass moment of inertia of wind tunnel model compared to full-scale structure for torsion.

Config.	$I_{e,FS}$ [kgm^2/m]	$I_{e,MS,target}$ [kgm^2/m]	$I_{e,MS}$ [kgm^2/m]	Deviation [%]
1	242752	0.039	0.036	7.54-6.93
2a	350052	0.056	0.053	5.04
2b	350052	0.056	0.056	0.61
2d	350052	0.056	0.056	0.81
3	242752	0.039	0.036-0.037	7.12-5.92
4	350052	0.056	0.054	3.82

The normalised data represents full-scale values for a structure, where modal mass, mode shapes, damping ratio, etc. correspond to model conditions.

The mass-damping parameters as defined in equations (6.3) and (6.4) of the main report, are listed in the tables below along with the main results.

Table D.4: Dynamic properties for vertical vortex-induced vibrations and general mass-damping parameters of the section models and the full scale structure.

Config.	δ [% LD]	$Sc_{G,H}$ [-]	Vortex-induced vibrations	$U_{crit,FS}$ [m/s]	St [-]	Heave, r/h [-]	$a_{FS,H}$ [m/s^2]
1	0.8	2.59	Yes	4.02	0.13	0.055	0.21
1	2.0	6.24	Yes	3.35	0.16	0.019	0.07
1	3.6	11.7	No	-	-	-	-
2a	1.7	5.57	Yes	5.27	0.10	0.061	0.23
2a	2.6	9.40	No	-	-	-	-
2a	3.6	12.5	No	-	-	-	-
2b	1.6	5.47	No	-	-	-	-
2c	1.9	6.62	Yes	6.17	0.09	0.076	0.29
2d	1.9	6.62	Yes	6.77	0.08	0.039	0.15
3	0.8	2.59	Yes	4.01	0.13	0.063	0.24
3	1.9	5.93	Yes	4.08	0.13	0.018	0.07
3	3.6	11.7	No	-	-	-	-
4	1.9	6.41	No	-	-	-	-

Table D.5: Dynamic properties for torsional vortex-induced vibrations and general mass-damping parameters of the section models and the full scale structure.

Config.	δ [% LD]	$Sc_{G,T}$ [-]	Vortex-induced vibrations	$U_{crit,FS}$ [m/s]	St [-]	Torsion, Φ [°]	$a_{FS,T}$ [m/s^2]
1	0.6	0.99	Yes	14.7	0.12	1.04	1.81
1	1.8	3.00	No	-	-	-	-
2a	0.8	1.96	Yes	13.9	0.11	0.30	0.41
2b	1.1	2.86	No	-	-	-	-
2d	0.9	2.34	Yes	17.9	0.08	0.30	0.40
3	0.7	1.17	Yes	15.3	0.11	0.64	1.10
3	1.1	1.85	Yes	14.9	0.11	0.19	0.32
3	1.5	2.53	No	-	-	-	-
4	1.4	3.48	No	-	-	-	-

In order to translate the data from the tables and plots in the following pages, the frequencies and normalisation height are needed. These are listed in the table below.

Table D.6: Vertical frequency n_H, torsional frequency n_T, and normalisation height h of full scale structure.

Config.	n_H [Hz]	n_T [Hz]	h [m]
1, 3	0.18	0.57	3.00
2a, 2b, 2c, 2d, 4	0.18	0.50	3.00

D.1 (1) PRESENT BRIDGE

D.1.1 (1) Heaving vibrations – 0.8% damping
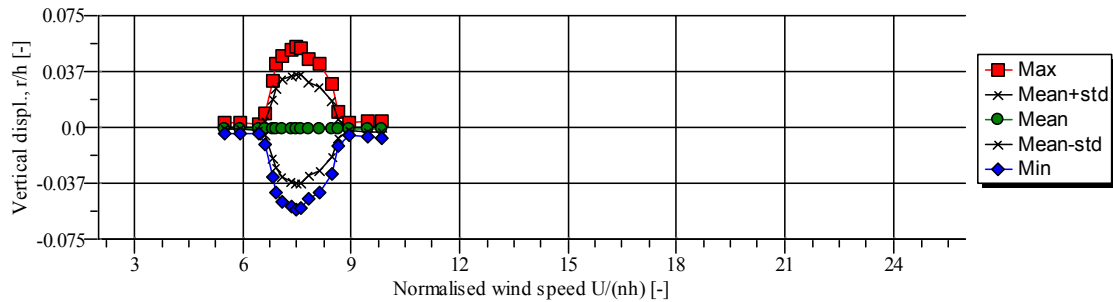
$U/(n_H h)$ [-]	Vertical displacement, r/h [-]			
	Mean	Std	Max	Min
5.49	-0.0006	0.0008	0.0027	-0.0039
5.92	-0.0007	0.0008	0.0026	-0.0043
6.45	-0.0008	0.0008	0.0024	-0.0039
6.60	-0.0008	0.0047	0.0092	-0.0114
6.82	-0.0008	0.0200	0.0314	-0.0331
6.91	-0.0007	0.0268	0.0430	-0.0439
7.09	-0.0007	0.0327	0.0483	-0.0496
7.35	-0.0008	0.0353	0.0518	-0.0536
7.45	-0.0009	0.0368	0.0539	-0.0552
7.62	-0.0010	0.0365	0.0532	-0.0547
7.82	-0.0010	0.0312	0.0462	-0.0479
8.11	-0.0010	0.0284	0.0424	-0.0442
8.44	-0.0010	0.0190	0.0293	-0.0315
8.63	-0.0011	0.0058	0.0106	-0.0122
8.92	-0.0011	0.0010	0.0028	-0.0053
9.43	-0.0012	0.0016	0.0040	-0.0065
9.86	-0.0013	0.0017	0.0043	-0.0072

Figure D.1: Heaving response of configuration 1 (present bridge). Low turbulent flow. Structural damping: approx. 0.8% LD. n is the heaving frequency.

D.1.2 (1) Heaving vibrations – 2.0% damping
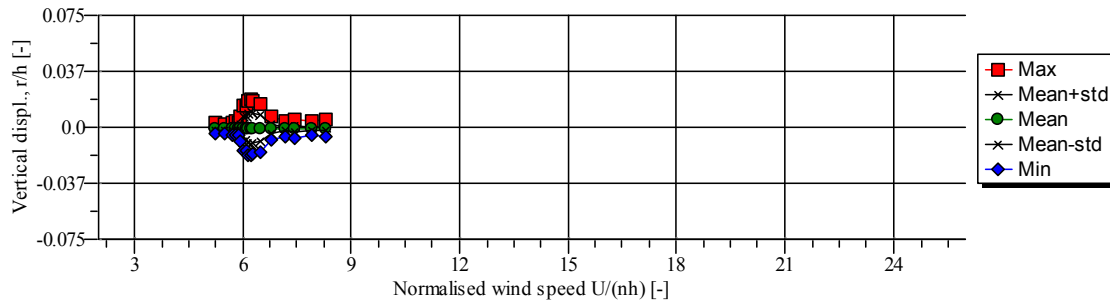
$U/(n_H h)$ [-]	Vertical displacement, r/h [-]			
	Mean	Std	Max	Min
5.24	-0.0008	0.0008	0.0029	-0.0047
5.49	-0.0009	0.0008	0.0026	-0.0045
5.71	-0.0009	0.0008	0.0030	-0.0049
5.78	-0.0008	0.0010	0.0038	-0.0048
5.89	-0.0009	0.0013	0.0035	-0.0055
5.92	-0.0008	0.0034	0.0075	-0.0094
5.99	-0.0008	0.0081	0.0141	-0.0158
6.08	-0.0008	0.0076	0.0147	-0.0154
6.13	-0.0008	0.0101	0.0177	-0.0189
6.21	-0.0008	0.0110	0.0187	-0.0193
6.27	-0.0008	0.0099	0.0172	-0.0179
6.49	-0.0008	0.0089	0.0151	-0.0167
6.77	-0.0008	0.0032	0.0070	-0.0087
7.17	-0.0008	0.0014	0.0042	-0.0059
7.42	-0.0009	0.0017	0.0053	-0.0075
7.91	-0.0010	0.0012	0.0037	-0.0056
8.30	-0.0010	0.0013	0.0051	-0.0067

Figure D.2: Heaving response of configuration 1 (present bridge). Low turbulent flow. Structural damping: approx. 2.0% LD. n is the heaving frequency.

D.1.3 (1) Heaving vibrations – 3.6% damping
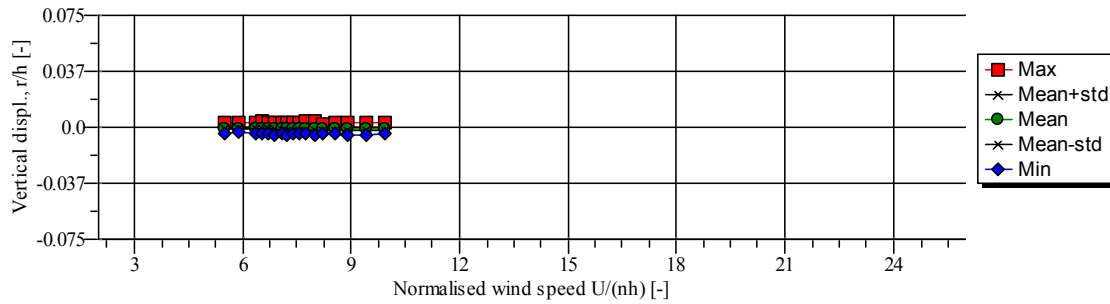
$U/(n_H h)$ [-]	Vertical displacement, r/h [-]			
	Mean	Std	Max	Min
5.51	-0.0006	0.0008	0.0027	-0.0041
5.89	-0.0006	0.0008	0.0030	-0.0036
6.37	-0.0006	0.0009	0.0027	-0.0042
6.51	-0.0006	0.0009	0.0040	-0.0041
6.70	-0.0007	0.0009	0.0027	-0.0041
6.89	-0.0006	0.0009	0.0029	-0.0049
7.07	-0.0007	0.0009	0.0034	-0.0046
7.19	-0.0007	0.0010	0.0031	-0.0047
7.40	-0.0007	0.0010	0.0031	-0.0047
7.58	-0.0007	0.0010	0.0030	-0.0041
7.72	-0.0007	0.0011	0.0042	-0.0045
8.01	-0.0008	0.0010	0.0039	-0.0051
8.21	-0.0008	0.0009	0.0026	-0.0043
8.57	-0.0009	0.0009	0.0027	-0.0045
8.91	-0.0009	0.0010	0.0029	-0.0047
9.41	-0.0009	0.0009	0.0026	-0.0048
9.92	-0.0011	0.0010	0.0034	-0.0047

Figure D.3: Heaving response of configuration 1 (present bridge). Low turbulent flow. Structural damping: approx. 3.6% LD. n is the heaving frequency

D.1.4 (1) Torsional vibrations – 0.6% damping
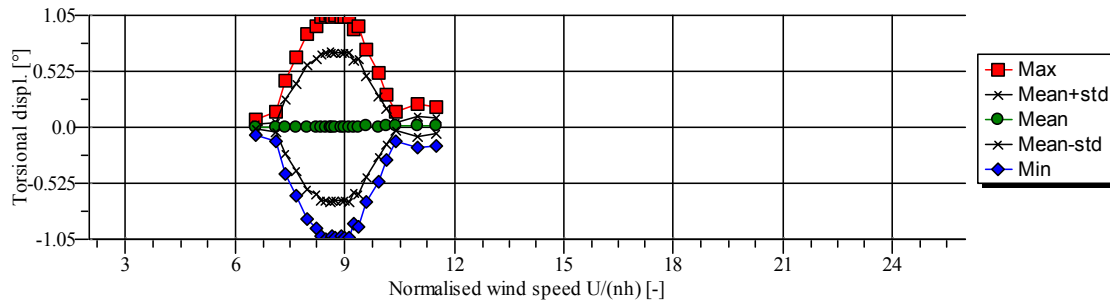
$U/(n_T h)$ [-]	Torsional displacement, Φ [°]			
	Mean	Std	Max	Min
6.56	0.0024	0.0196	0.0775	-0.0759
7.11	0.0028	0.0482	0.1431	-0.1316
7.36	0.0036	0.2566	0.4377	-0.4354
7.67	0.0041	0.4108	0.6611	-0.6401
7.96	0.0049	0.5824	0.8727	-0.8606
8.24	0.0050	0.6322	0.9536	-0.9481
8.37	0.0044	0.6862	1.0381	-1.0265
8.46	0.0044	0.6924	1.0482	-1.0485
8.60	0.0051	0.7109	1.0679	-1.0442
8.65	0.0050	0.6922	1.0333	-1.0202
8.76	0.0053	0.6935	1.0466	-1.0291
8.90	0.0053	0.6946	1.0358	-1.0211
9.00	0.0057	0.6947	1.0384	-1.0291
9.11	0.0057	0.7011	1.0383	-1.0327
9.23	0.0066	0.6144	0.9193	-0.9106
9.36	0.0066	0.6391	0.9531	-0.9355
9.61	0.0077	0.4678	0.7252	-0.6954
9.93	0.0071	0.2911	0.5079	-0.5062
10.16	0.0088	0.1699	0.3132	-0.3016
10.42	0.0088	0.0410	0.1488	-0.1269
10.99	0.0093	0.0922	0.2196	-0.1829
11.50	0.0099	0.0745	0.1830	-0.1682

Figure D.4: Torsional response of configuration 1 (present bridge). Low turbulent flow. Structural damping: approx. 0.6% LD. n is the torsional frequency.

D.1.5 (1) Torsional vibrations – 1.8% damping
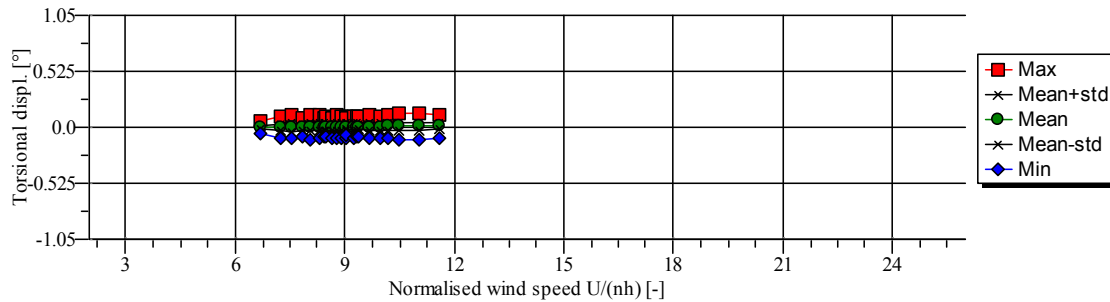
$U/(n_Th)$ [-]	Torsional displacement, Φ [°]			
	Mean	Std	Max	Min
6.70	0.0031	0.0160	0.0592	-0.0618
7.23	0.0032	0.0333	0.1072	-0.0992
7.55	0.0040	0.0456	0.1100	-0.1059
7.82	0.0043	0.0301	0.0913	-0.0884
8.04	0.0039	0.0380	0.1178	-0.1104
8.31	0.0048	0.0413	0.1108	-0.0961
8.45	0.0056	0.0310	0.0920	-0.0833
8.47	0.0050	0.0308	0.1011	-0.0922
8.64	0.0051	0.0285	0.0894	-0.0959
8.79	0.0056	0.0383	0.1097	-0.1085
8.90	0.0059	0.0331	0.1053	-0.1057
9.01	0.0061	0.0408	0.1057	-0.0989
9.05	0.0061	0.0264	0.0870	-0.0762
9.23	0.0066	0.0342	0.1022	-0.0990
9.33	0.0063	0.0314	0.1061	-0.0909
9.36	0.0061	0.0277	0.1052	-0.0865
9.67	0.0071	0.0336	0.1104	-0.1037
9.96	0.0072	0.0344	0.1044	-0.0960
10.20	0.0073	0.0408	0.1141	-0.1018
10.50	0.0077	0.0362	0.1317	-0.1122
11.04	0.0082	0.0396	0.1281	-0.1128
11.58	0.0092	0.0284	0.1183	-0.0971

Figure D.5: Torsional response of configuration 1 (present bridge). Low turbulent flow. Structural damping: approx. 1.8% LD. n is the torsional frequency.

Askoy Bridge
Wind tunnel tests and analyses
Annex D
Vortex-induced vibrations, section model 1:50
Revision 0, December 2014

D.2   (2a) ONE WALKWAY UPSTREAM.

D.2.1 (2a) Heaving vibrations – 1.7% damping
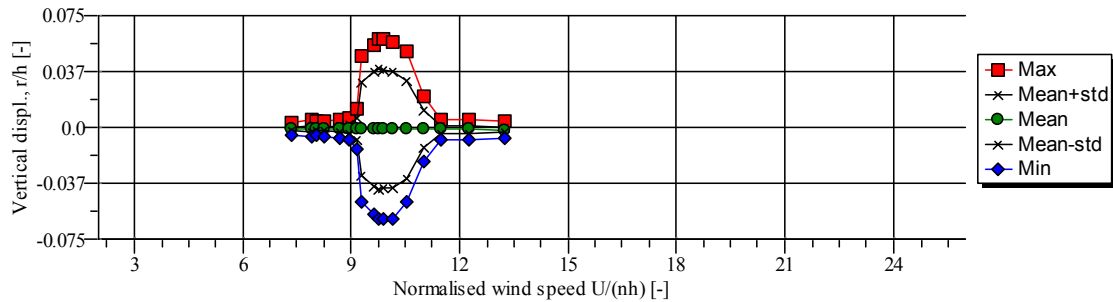
$U/(n_H h)$ [-]	Vertical displacement, r/h [-]			
	Mean	Std	Max	Min
7.32	-0.0009	0.0010	0.0026	-0.0048
7.90	-0.0010	0.0017	0.0048	-0.0059
8.05	-0.0010	0.0012	0.0037	-0.0049
8.26	-0.0011	0.0013	0.0043	-0.0061
8.67	-0.0011	0.0022	0.0050	-0.0071
8.94	-0.0012	0.0028	0.0058	-0.0081
9.13	-0.0012	0.0070	0.0128	-0.0150
9.28	-0.0012	0.0310	0.0475	-0.0504
9.61	-0.0011	0.0383	0.0556	-0.0583
9.75	-0.0011	0.0405	0.0589	-0.0610
9.90	-0.0013	0.0397	0.0589	-0.0610
10.12	-0.0013	0.0391	0.0577	-0.0613
10.53	-0.0014	0.0326	0.0506	-0.0505
10.99	-0.0014	0.0126	0.0206	-0.0233
11.49	-0.0014	0.0023	0.0053	-0.0079
12.25	-0.0015	0.0025	0.0052	-0.0086
13.26	-0.0017	0.0019	0.0040	-0.0073

Figure D.6: Heaving response of configuration 2a (one walkway upstream). Low turbulent flow. Structural damping: approx. 1.7% LD. n is the heaving frequency.

Askoy Bridge
Wind tunnel tests and analyses   Annex D   Revision 0, December 2014
                     Vortex-induced vibrations, section model 1:50

D.2.2 (2a) Heaving vibrations – 2.6% damping
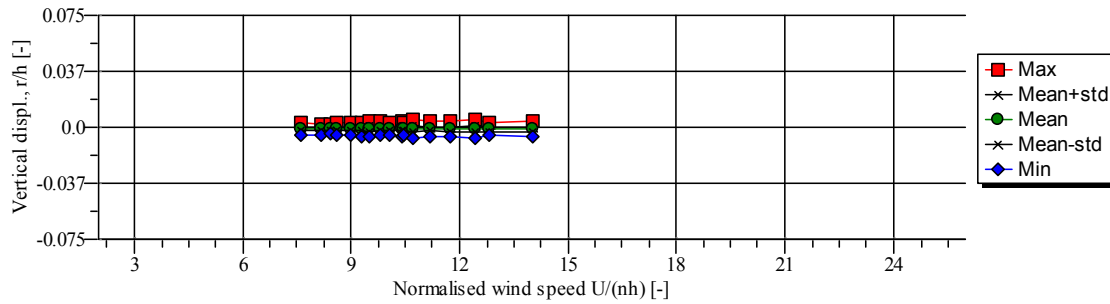
$U/(n_H h)$ [-]	Vertical displacement, r/h [-]			
	Mean	Std	Max	Min
7.59	-0.0009	0.0010	0.0031	-0.0055
8.18	-0.0010	0.0008	0.0025	-0.0047
8.42	-0.0010	0.0008	0.0025	-0.0040
8.58	-0.0010	0.0011	0.0031	-0.0050
8.96	-0.0010	0.0011	0.0030	-0.0051
9.30	-0.0010	0.0012	0.0031	-0.0059
9.50	-0.0010	0.0016	0.0041	-0.0058
9.80	-0.0010	0.0012	0.0040	-0.0055
10.07	-0.0010	0.0012	0.0035	-0.0055
10.41	-0.0010	0.0014	0.0038	-0.0061
10.44	-0.0010	0.0013	0.0033	-0.0052
10.71	-0.0010	0.0020	0.0054	-0.0073
11.19	-0.0011	0.0012	0.0042	-0.0060
11.74	-0.0012	0.0016	0.0037	-0.0062
12.43	-0.0012	0.0021	0.0052	-0.0078
12.83	-0.0012	0.0014	0.0035	-0.0057
14.03	-0.0013	0.0014	0.0037	-0.0064

Figure D.7: Heaving response of configuration 2a (one walkway upstream). Low turbulent flow. Structural damping: approx. 2.6% LD. n is the heaving frequency.

D.2.3 (2a) Heaving vibrations – 3.6% damping
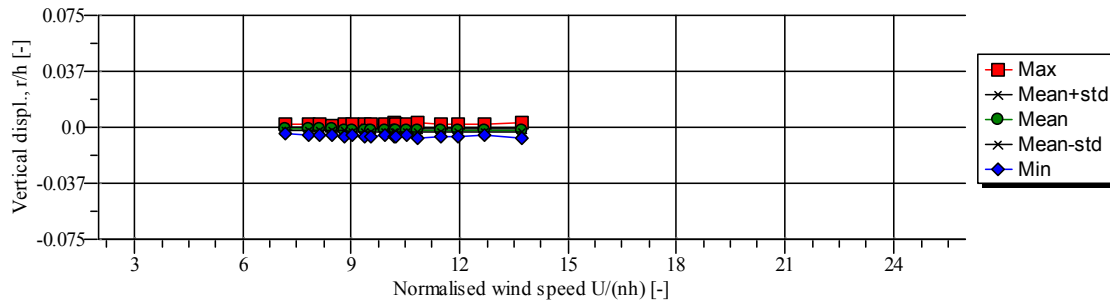
$U/(n_H h)$ [-]	Vertical displacement, r/h [-]			
	Mean	Std	Max	Min
7.16	-0.0011	0.0008	0.0021	-0.0040
7.81	-0.0013	0.0009	0.0020	-0.0048
8.11	-0.0014	0.0008	0.0016	-0.0048
8.44	-0.0015	0.0008	0.0015	-0.0050
8.82	-0.0016	0.0009	0.0024	-0.0068
9.02	-0.0017	0.0010	0.0025	-0.0055
9.35	-0.0018	0.0012	0.0025	-0.0067
9.54	-0.0018	0.0011	0.0025	-0.0060
9.91	-0.0018	0.0010	0.0021	-0.0057
10.18	-0.0019	0.0012	0.0027	-0.0061
10.25	-0.0019	0.0009	0.0021	-0.0060
10.53	-0.0019	0.0008	0.0018	-0.0055
10.83	-0.0019	0.0013	0.0032	-0.0069
11.47	-0.0020	0.0011	0.0022	-0.0060
11.94	-0.0020	0.0013	0.0024	-0.0067
12.70	-0.0021	0.0011	0.0023	-0.0057
13.71	-0.0022	0.0013	0.0030	-0.0075

Figure D.8: Heaving response of configuration 2a (one walkway upstream). Low turbulent flow. Structural damping: approx. 3.6% LD. n is the heaving frequency.

D.2.4 (2a) Torsional vibrations – 0.8% damping
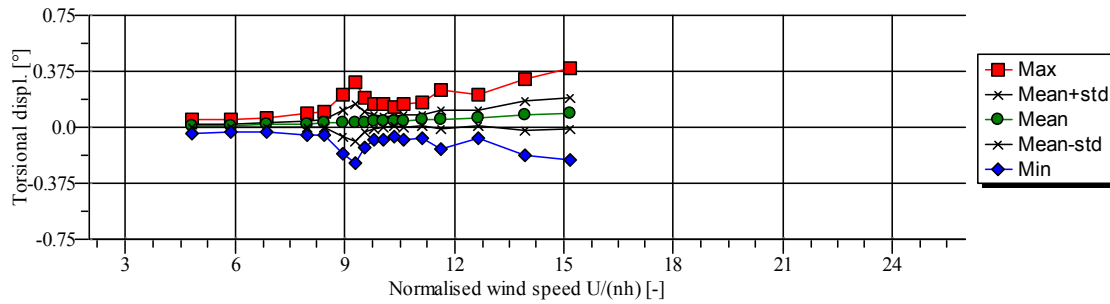
$U/(n_Th)$ [-]	Torsional displacement, Φ [°]			
	Mean	Std	Max	Min
4.81	0.0076	0.0108	0.0509	-0.0394
5.89	0.0114	0.0115	0.0542	-0.0299
6.87	0.0166	0.0124	0.0658	-0.0309
7.98	0.0231	0.0223	0.0941	-0.0512
8.44	0.0269	0.0236	0.0996	-0.0483
8.96	0.0300	0.0883	0.2229	-0.1722
9.27	0.0324	0.1278	0.3049	-0.2368
9.54	0.0351	0.0641	0.1975	-0.1307
9.79	0.0368	0.0433	0.1578	-0.0818
10.05	0.0390	0.0344	0.1546	-0.0847
10.37	0.0412	0.0303	0.1362	-0.0594
10.59	0.0435	0.0424	0.1589	-0.0809
11.14	0.0480	0.0390	0.1629	-0.0774
11.63	0.0530	0.0618	0.2468	-0.1409
12.66	0.0639	0.0485	0.2142	-0.0722
13.93	0.0786	0.0992	0.3223	-0.1837
15.18	0.0948	0.1032	0.3955	-0.2177

Figure D.9: Torsional response of configuration 2a (one walkway upstream). Low turbulent flow. Structural damping: approx. 0.8% LD. n is the torsional frequency.

D.2.5 (2a) Torsional vibrations – 1.9% damping
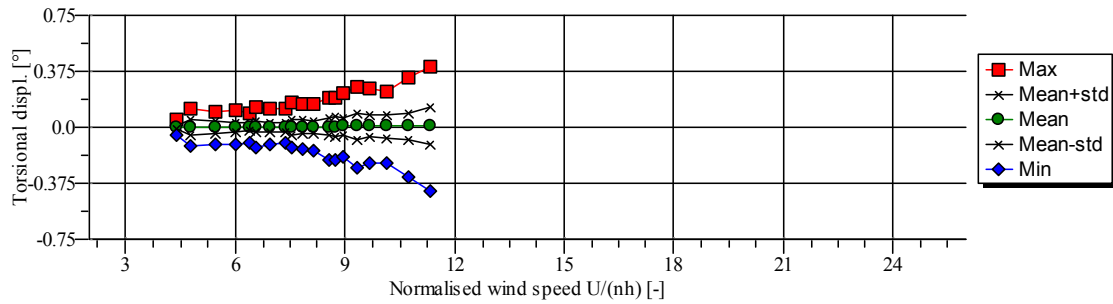
$U/(n_T h)$ [-]	Torsional displacement, Φ [°]			
	Mean	Std	Max	Min
4.39	0.0001	0.0149	0.0548	-0.0548
4.76	0.0005	0.0500	0.1251	-0.1241
5.46	0.0003	0.0380	0.1088	-0.1131
6.02	0.0022	0.0324	0.1162	-0.1187
6.40	0.0015	0.0253	0.0912	-0.1024
6.58	0.0018	0.0377	0.1323	-0.1303
6.95	0.0020	0.0286	0.1240	-0.1134
7.38	0.0031	0.0297	0.1205	-0.1079
7.54	0.0025	0.0511	0.1633	-0.1398
7.83	0.0039	0.0488	0.1511	-0.1446
8.16	0.0033	0.0420	0.1519	-0.1590
8.58	0.0050	0.0600	0.1978	-0.2136
8.73	0.0042	0.0651	0.2008	-0.2160
8.96	0.0052	0.0558	0.2269	-0.1943
9.35	0.0057	0.0905	0.2677	-0.2657
9.69	0.0068	0.0729	0.2555	-0.2396
10.13	0.0063	0.0801	0.2448	-0.2376
10.75	0.0061	0.0860	0.3336	-0.3365
11.33	0.0071	0.1259	0.4016	-0.4249

Figure D.10: Torsional response of configuration 2a (one walkway upstream). Low turbulent flow. Structural damping: approx. 1.9% LD. n is the torsional frequency.

D.3 (2b) ONE WALKWAY DOWNSTREAM

D.3.1 (2b) Heaving vibrations – 1.6% damping
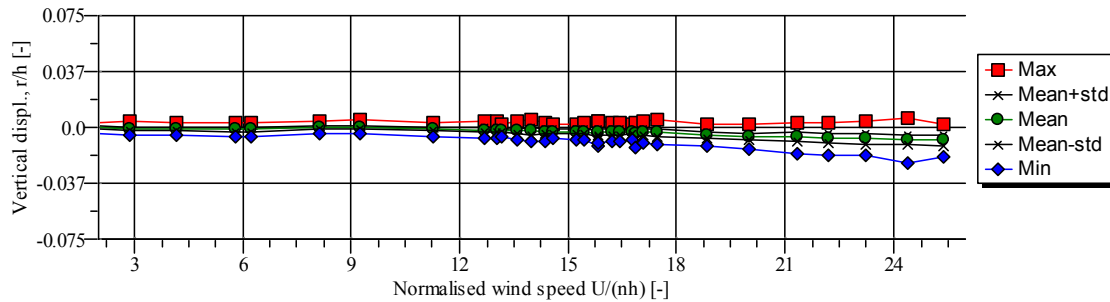
$U/(n_H h)$ [-]	Vertical displacement, r/h [-]			
	Mean	Std	Max	Min
1.34	-0.0002	0.0011	0.0037	-0.0043
1.50	-0.0002	0.0009	0.0034	-0.0039
2.87	-0.0006	0.0009	0.0037	-0.0049
4.16	-0.0010	0.0009	0.0028	-0.0050
5.80	-0.0014	0.0012	0.0035	-0.0065
6.22	-0.0015	0.0012	0.0030	-0.0062
8.13	0.0004	0.0011	0.0044	-0.0040
9.22	-0.0002	0.0010	0.0054	-0.0042
11.25	-0.0011	0.0012	0.0036	-0.0058
12.67	-0.0017	0.0015	0.0038	-0.0072
13.03	-0.0018	0.0016	0.0037	-0.0077
13.59	-0.0023	0.0016	0.0041	-0.0078
13.98	-0.0024	0.0023	0.0053	-0.0096
14.60	-0.0026	0.0013	0.0022	-0.0074
15.21	-0.0028	0.0015	0.0025	-0.0083
15.45	-0.0029	0.0014	0.0035	-0.0082
15.84	-0.0029	0.0024	0.0042	-0.0106
16.24	-0.0031	0.0017	0.0036	-0.0091
16.43	-0.0032	0.0018	0.0030	-0.0096
16.80	-0.0033	0.0013	0.0021	-0.0082
17.48	-0.0035	0.0027	0.0053	-0.0119
18.86	-0.0055	0.0021	0.0017	-0.0128
20.00	-0.0059	0.0022	0.0019	-0.0146
21.33	-0.0066	0.0031	0.0034	-0.0176
22.21	-0.0070	0.0033	0.0035	-0.0184
23.25	-0.0075	0.0039	0.0037	-0.0191
24.39	-0.0081	0.0033	0.0059	-0.0236
25.39	-0.0088	0.0034	0.0021	-0.0202

Figure D.11: Heaving response of configuration 2b (one walkway downstream). Low turbulent flow. Structural damping: approx. 1.6% LD. n is the heaving frequency.

D.3.2 (2b) Torsional vibration – 1.1% damping
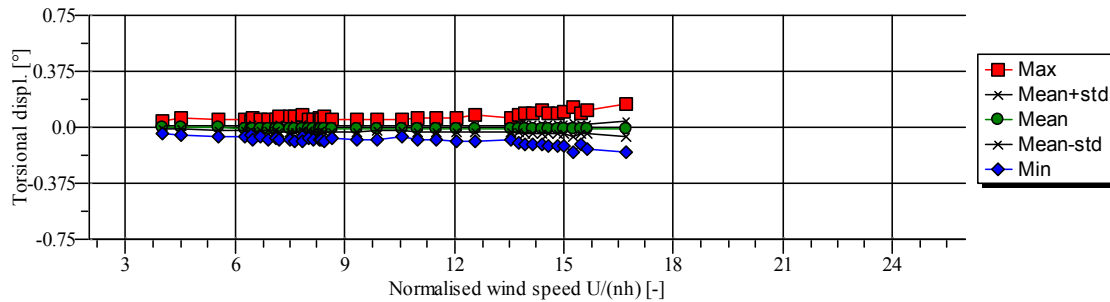
$U/(n_Th)$ [-]	Torsional displacement, Φ [°]			
	Mean	Std	Max	Min
3.99	-0.0027	0.0115	0.0382	-0.0455
4.53	-0.0031	0.0113	0.0627	-0.0488
5.55	-0.0045	0.0159	0.0505	-0.0646
6.25	-0.0053	0.0146	0.0485	-0.0642
6.43	-0.0056	0.0128	0.0442	-0.0567
6.50	-0.0060	0.0218	0.0648	-0.0796
6.71	-0.0070	0.0167	0.0554	-0.0631
6.90	-0.0070	0.0157	0.0480	-0.0800
7.10	-0.0075	0.0177	0.0533	-0.0688
7.22	-0.0074	0.0244	0.0677	-0.0808
7.52	-0.0078	0.0228	0.0680	-0.0850
7.83	-0.0098	0.0143	0.0456	-0.0638
8.35	-0.0095	0.0162	0.0501	-0.0799
9.33	-0.0098	0.0175	0.0515	-0.0786
9.90	-0.0092	0.0166	0.0546	-0.0796
10.56	-0.0096	0.0153	0.0536	-0.0670
11.51	-0.0094	0.0190	0.0654	-0.0818
12.08	-0.0103	0.0209	0.0658	-0.0916
12.58	-0.0094	0.0225	0.0785	-0.0889
13.54	-0.0108	0.0200	0.0629	-0.0846
13.95	-0.0106	0.0287	0.0950	-0.1111
14.17	-0.0110	0.0306	0.0948	-0.1103
14.55	-0.0108	0.0280	0.0967	-0.1283
14.82	-0.0111	0.0340	0.0941	-0.1198
15.00	-0.0110	0.0317	0.1046	-0.1225
15.26	-0.0108	0.0465	0.1378	-0.1644
15.64	-0.0114	0.0323	0.1182	-0.1504
16.69	-0.0118	0.0486	0.1568	-0.1626

Figure D.12: Torsional response of configuration 2b (one walkway downstream). Low turbulent flow. Structural damping: approx. 1.1% LD. n is the torsional frequency.

D.4   (2c) ONE WALKWAY UPSTREAM, GUIDE VANES

D.4.1   (2c) Heaving vibrations – 1.9% damping
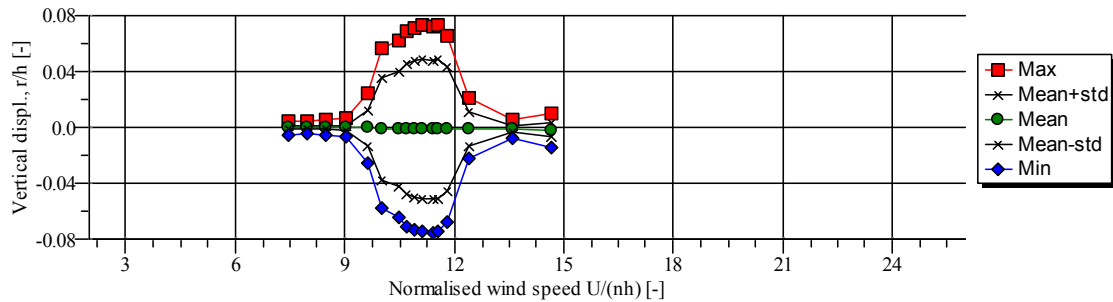
$U/(n_H h)$ [-]	Vertical displacement, r/h [-]			
	Mean	Std	Max	Min
7.44	-0.0003	0.0010	0.0044	-0.0054
7.97	-0.0002	0.0010	0.0050	-0.0049
8.47	-0.0001	0.0011	0.0051	-0.0052
9.05	-0.0002	0.0017	0.0063	-0.0068
9.63	-0.0005	0.0128	0.0249	-0.0256
10.02	-0.0010	0.0369	0.0566	-0.0576
10.48	-0.0010	0.0415	0.0623	-0.0643
10.68	-0.0010	0.0470	0.0688	-0.0712
10.89	-0.0010	0.0488	0.0715	-0.0738
11.13	-0.0011	0.0495	0.0730	-0.0748
11.42	-0.0012	0.0495	0.0726	-0.0755
11.53	-0.0011	0.0497	0.0732	-0.0749
11.80	-0.0011	0.0450	0.0660	-0.0680
12.42	-0.0011	0.0122	0.0206	-0.0224
13.59	-0.0009	0.0022	0.0060	-0.0076
14.65	-0.0017	0.0050	0.0104	-0.0147

Figure D.13: Heaving response of configuration 2c (one walkway upstream, guide vanes). Low turbulent flow. Structural damping: approx. 1.9% LD. n is the heaving frequency.

D.5 (2d) ONE WALKWAY UPSTREAM, GUIDE VANES, VORTEX SPOILER

D.5.1 (2d) Heaving vibrations – 1.9% damping
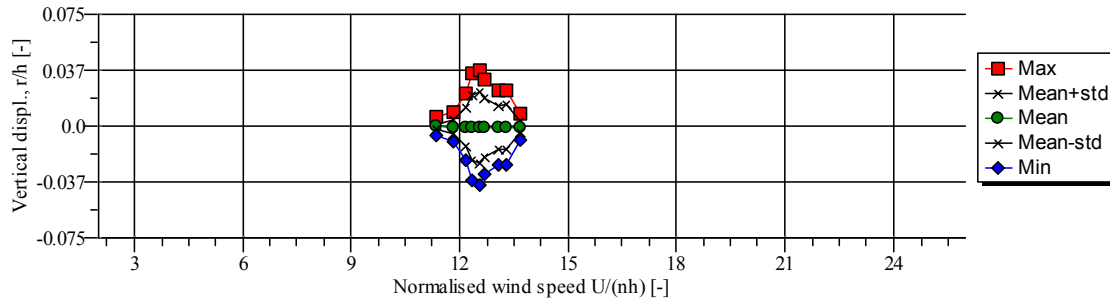
$U/(n_H h)$ [-]	Vertical displacement, r/h [-]			
	Mean	Std	Max	Min
11.35	-0.0004	0.0020	0.0060	-0.0067
11.83	-0.0006	0.0044	0.0097	-0.0108
12.16	-0.0006	0.0131	0.0222	-0.0232
12.36	-0.0009	0.0222	0.0350	-0.0366
12.54	-0.0009	0.0237	0.0376	-0.0392
12.67	-0.0009	0.0200	0.0311	-0.0327
13.09	-0.0008	0.0146	0.0237	-0.0261
13.30	-0.0008	0.0150	0.0240	-0.0265
13.69	-0.0007	0.0035	0.0088	-0.0094

Figure D.14: Heaving response of configuration 2d (one walkway upstream, guide vanes, vortex spoiler). Low turbulent flow. Structural damping: approx. 1.9% LD. n is the heaving frequency.

D.5.2 (2d) Torsional vibrations – 0.9% damping
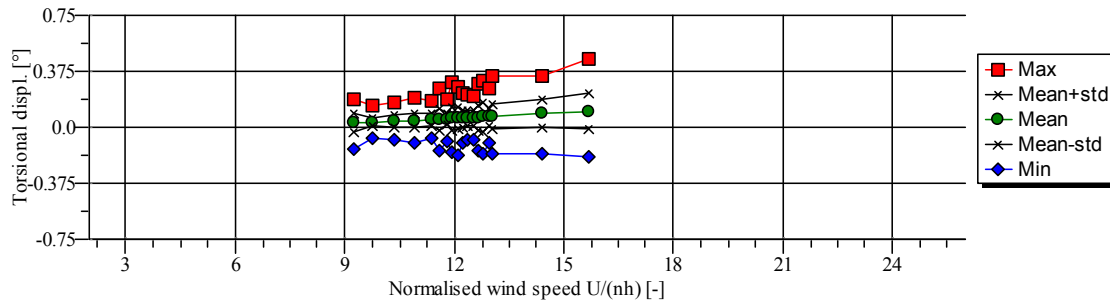
$U/(n_T h)$ [-]	Torsional displacement, Φ [°]			
	Mean	Std	Max	Min
9.24	0.0309	0.0651	0.1914	-0.1424
9.77	0.0361	0.0292	0.1460	-0.0762
10.37	0.0418	0.0413	0.1682	-0.0830
10.90	0.0466	0.0509	0.1993	-0.1064
11.38	0.0516	0.0403	0.1755	-0.0744
11.59	0.0540	0.0726	0.2656	-0.1574
11.80	0.0565	0.0379	0.1878	-0.0897
11.93	0.0581	0.0808	0.2988	-0.1717
12.08	0.0599	0.0721	0.2734	-0.1835
12.22	0.0604	0.0593	0.2268	-0.1034
12.36	0.0643	0.0501	0.2169	-0.0843
12.52	0.0657	0.0520	0.2116	-0.0860
12.65	0.0673	0.0834	0.2965	-0.1522
12.78	0.0688	0.0975	0.3111	-0.1724
12.96	0.0701	0.0560	0.2578	-0.1066
13.06	0.0723	0.0827	0.3485	-0.1823
14.39	0.0905	0.0935	0.3434	-0.1733
15.69	0.1089	0.1189	0.4590	-0.1969

Figure D.15: Torsional response of configuration 2d (one walkway upstream, guide vanes, vortex spoielr). Low turbulent flow. Structural damping: approx. 0.9% LD. n is the torsional frequency.

Askoy Bridge
Wind tunnel tests and analyses
Annex D
Vortex-induced vibrations, section model 1:50
Revision 0, December 2014

D.6 (3) PRESENT BRIDGE, MODIFIED RAILINGS

D.6.1 (3) Heaving vibrations – 0.8% damping
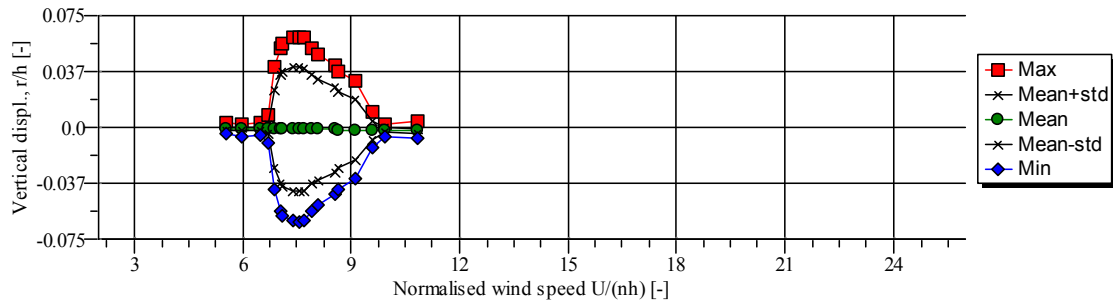
$U/(n_H h)$ [-]	Vertical displacement, r/h [-]			
	Mean	Std	Max	Min
5.52	-0.0008	0.0008	0.0028	-0.0042
5.96	-0.0009	0.0008	0.0026	-0.0059
6.47	-0.0010	0.0008	0.0026	-0.0048
6.70	-0.0011	0.0035	0.0084	-0.0109
6.85	-0.0011	0.0263	0.0405	-0.0418
7.03	-0.0012	0.0365	0.0534	-0.0560
7.10	-0.0013	0.0387	0.0564	-0.0589
7.38	-0.0013	0.0420	0.0607	-0.0629
7.55	-0.0014	0.0418	0.0603	-0.0633
7.68	-0.0014	0.0411	0.0606	-0.0627
7.89	-0.0015	0.0364	0.0527	-0.0562
8.09	-0.0015	0.0338	0.0486	-0.0521
8.54	-0.0015	0.0283	0.0415	-0.0450
8.65	-0.0016	0.0255	0.0374	-0.0412
9.09	-0.0017	0.0207	0.0313	-0.0344
9.59	-0.0018	0.0063	0.0100	-0.0134
9.94	-0.0019	0.0014	0.0022	-0.0066
10.83	-0.0021	0.0016	0.0037	-0.0072

Figure D.16: Heaving response of configuration 3 (present bridge with modified railings). Low turbulent flow. Structural damping: approx. 0.8% LD. n is the heaving frequency.

D.6.2 (3) Heaving vibrations – 1.9% damping
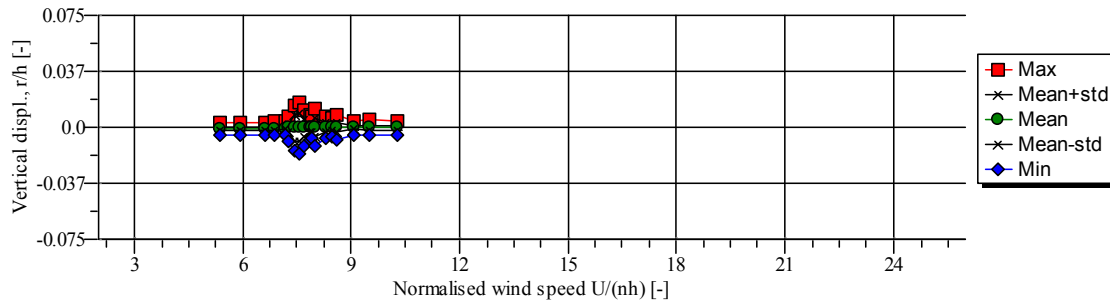
$U/(n_H h)$ [-]	Vertical displacement, r/h [-]			
	Mean	Std	Max	Min
5.38	-0.0009	0.0009	0.0029	-0.0048
5.94	-0.0009	0.0009	0.0029	-0.0048
6.61	-0.0008	0.0010	0.0032	-0.0050
6.86	-0.0007	0.0010	0.0036	-0.0053
7.19	-0.0006	0.0010	0.0039	-0.0051
7.24	-0.0005	0.0030	0.0072	-0.0094
7.45	-0.0005	0.0084	0.0145	-0.0157
7.56	-0.0004	0.0094	0.0166	-0.0178
7.70	-0.0004	0.0054	0.0111	-0.0123
7.85	-0.0004	0.0026	0.0079	-0.0087
7.91	-0.0003	0.0028	0.0073	-0.0072
7.98	-0.0002	0.0060	0.0121	-0.0121
8.28	-0.0002	0.0029	0.0077	-0.0077
8.47	-0.0003	0.0017	0.0058	-0.0064
8.60	-0.0002	0.0032	0.0079	-0.0081
9.08	-0.0003	0.0011	0.0043	-0.0049
9.52	-0.0003	0.0016	0.0050	-0.0057
10.29	-0.0005	0.0012	0.0041	-0.0050

Figure D.17: Heaving response of configuration 3 (present bridge with modified railings). Low turbulent flow. Structural damping: approx. 1.9% LD. n is the heaving frequency.

D.6.3 (3) Heaving vibrations – 3.6% damping
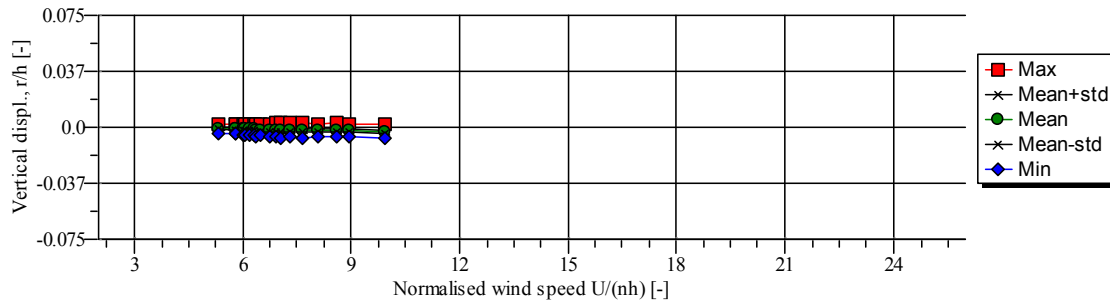
$U/(n_H h)$ [-]	Vertical displacement, r/h [-]			
	Mean	Std	Max	Min
5.30	-0.0008	0.0007	0.0024	-0.0044
5.79	-0.0010	0.0007	0.0020	-0.0042
5.79	-0.0011	0.0008	0.0022	-0.0045
6.01	-0.0013	0.0009	0.0024	-0.0049
6.03	-0.0014	0.0008	0.0022	-0.0050
6.20	-0.0015	0.0009	0.0025	-0.0057
6.30	-0.0016	0.0009	0.0024	-0.0057
6.36	-0.0017	0.0010	0.0025	-0.0059
6.49	-0.0017	0.0009	0.0024	-0.0055
6.74	-0.0018	0.0009	0.0017	-0.0062
6.92	-0.0018	0.0011	0.0029	-0.0060
7.04	-0.0019	0.0011	0.0027	-0.0069
7.30	-0.0020	0.0011	0.0031	-0.0061
7.65	-0.0021	0.0011	0.0026	-0.0069
8.06	-0.0022	0.0011	0.0024	-0.0065
8.59	-0.0023	0.0011	0.0027	-0.0065
8.92	-0.0024	0.0011	0.0022	-0.0064
9.93	-0.0027	0.0011	0.0022	-0.0069

Figure D.18: Heaving response of configuration 3 (present bridge with modified railings). Low turbulent flow. Structural damping: approx. 3.6% LD. n is the heaving frequency.

D.6.4 (3) Torsional vibrations – 0.7% damping
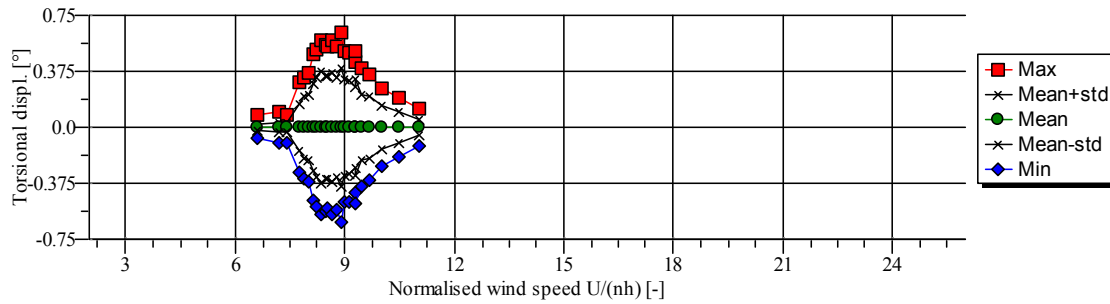
$U/(n_T h)$ [-]	Torsional displacement, Φ [°]			
	Mean	Std	Max	Min
6.60	-0.0007	0.0173	0.0801	-0.0737
7.20	-0.0009	0.0326	0.1064	-0.0994
7.41	-0.0007	0.0303	0.0863	-0.1003
7.75	-0.0014	0.1594	0.3027	-0.3006
7.87	-0.0016	0.2048	0.3355	-0.3432
8.01	-0.0005	0.2155	0.3651	-0.3671
8.16	-0.0010	0.2920	0.4885	-0.4866
8.23	-0.0014	0.3327	0.5247	-0.5281
8.34	0.0001	0.3796	0.5824	-0.5844
8.49	-0.0010	0.3430	0.5542	-0.5612
8.51	-0.0001	0.3480	0.5400	-0.5425
8.67	-0.0003	0.3635	0.5883	-0.5827
8.80	-0.0004	0.3347	0.5461	-0.5473
8.93	-0.0009	0.3933	0.6312	-0.6355
9.00	-0.0003	0.3193	0.5103	-0.5035
9.13	-0.0005	0.3093	0.4989	-0.4956
9.28	-0.0004	0.2717	0.4407	-0.4368
9.28	0.0016	0.3265	0.5139	-0.5110
9.44	0.0000	0.2188	0.3926	-0.3954
9.67	0.0002	0.2073	0.3542	-0.3564
10.01	0.0002	0.1427	0.2587	-0.2553
10.50	0.0000	0.0999	0.1962	-0.2001
11.04	0.0000	0.0484	0.1225	-0.1279

Figure D.19: Torsional response of configuration 3 (present bridge with modified railings). Low turbulent flow. Structural damping: approx. 0.7% LD. n is the torsional frequency.

D.6.5 (3) Torsional vibrations – 1.1% damping
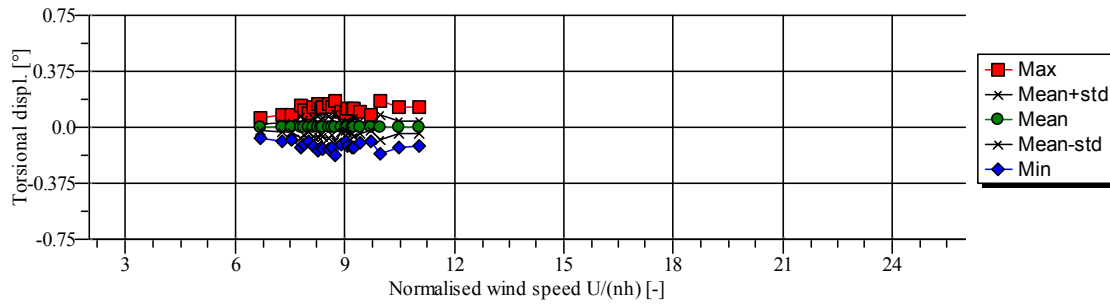
$U/(n_T h)$ [-]	Torsional displacement, Φ [°]			
	Mean	Std	Max	Min
6.70	0.0003	0.0185	0.0673	-0.0721
7.28	-0.0001	0.0297	0.0879	-0.0906
7.54	0.0002	0.0267	0.0869	-0.0812
7.81	-0.0003	0.0705	0.1462	-0.1406
7.87	0.0003	0.0483	0.1094	-0.1164
8.02	0.0005	0.0277	0.0904	-0.0912
8.14	0.0007	0.0588	0.1364	-0.1284
8.26	0.0012	0.0679	0.1603	-0.1533
8.36	0.0003	0.0562	0.1220	-0.1390
8.41	0.0006	0.0631	0.1396	-0.1422
8.57	0.0004	0.0682	0.1551	-0.1485
8.65	0.0007	0.0546	0.1380	-0.1337
8.72	0.0003	0.0937	0.1736	-0.1851
8.89	-0.0001	0.0350	0.1026	-0.1102
9.02	0.0002	0.0260	0.0919	-0.0890
9.07	-0.0001	0.0460	0.1255	-0.1297
9.19	0.0001	0.0455	0.1271	-0.1326
9.27	-0.0005	0.0606	0.1295	-0.1387
9.40	-0.0003	0.0386	0.1046	-0.1065
9.69	0.0003	0.0248	0.0807	-0.0955
9.98	0.0004	0.0843	0.1809	-0.1822
10.46	-0.0003	0.0414	0.1340	-0.1305
11.05	-0.0002	0.0442	0.1344	-0.1199

Figure D.20: Torsional response of configuration 3 (present bridge with modified railings). Low turbulent flow. Structural damping: approx. 1.1% LD. n is the torsional frequency.

Askoy Bridge
Wind tunnel tests and analyses
Annex D
Vortex-induced vibrations, section model 1:50
Revision 0, December 2014

D.6.6 (3) Torsional vibrations – 1.5% damping
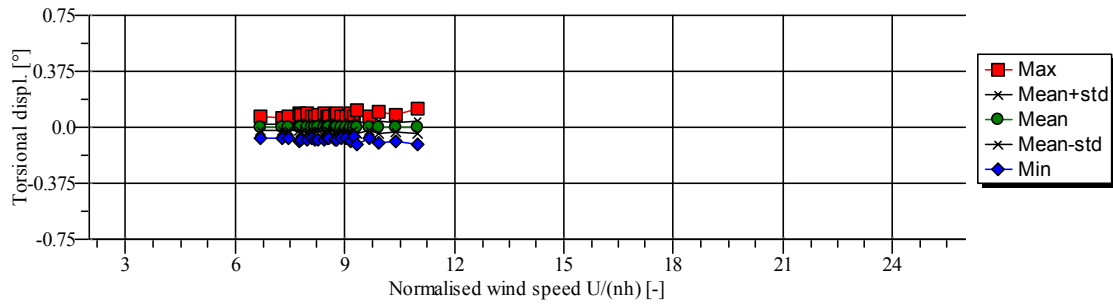
$U/(n_T h)$ [-]	Torsional displacement, Φ [°]			
	Mean	Std	Max	Min
6.70	-0.0006	0.0176	0.0682	-0.0679
7.28	-0.0008	0.0201	0.0647	-0.0742
7.47	-0.0010	0.0216	0.0689	-0.0761
7.75	-0.0007	0.0253	0.0903	-0.0914
7.82	-0.0003	0.0274	0.0819	-0.0844
7.95	-0.0007	0.0268	0.0912	-0.0878
8.08	-0.0003	0.0195	0.0750	-0.0725
8.18	-0.0001	0.0225	0.0744	-0.0790
8.28	-0.0004	0.0205	0.0816	-0.0843
8.43	-0.0004	0.0283	0.0891	-0.0871
8.51	0.0000	0.0188	0.0684	-0.0678
8.58	-0.0001	0.0216	0.0716	-0.0717
8.74	-0.0011	0.0283	0.0868	-0.0878
8.77	-0.0005	0.0313	0.0938	-0.0885
8.93	0.0001	0.0185	0.0698	-0.0711
9.02	-0.0002	0.0190	0.0679	-0.0725
9.16	-0.0002	0.0269	0.0897	-0.0895
9.26	-0.0006	0.0205	0.0718	-0.0673
9.34	-0.0003	0.0397	0.1149	-0.1155
9.66	-0.0002	0.0210	0.0753	-0.0767
9.91	-0.0008	0.0403	0.1009	-0.1014
10.42	-0.0004	0.0265	0.0867	-0.0893
11.01	-0.0010	0.0399	0.1214	-0.1182

Figure D.21: Torsional response of configuration 3 (present bridge with modified railings). Low turbulent flow. Structural damping: approx. 1.5% LD. n is the torsional frequency.

D.7 (4) TWO WALKWAYS

D.7.1 (4) Heaving vibrations – 1.9% damping
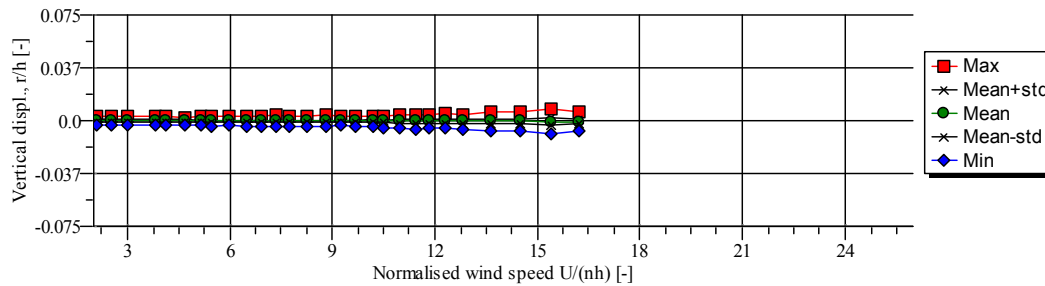
$U/(n_H h)$ [-]	Vertical displacement, r/h [-]			
	Mean	Std	Max	Min
1.50	0.0000	0.0007	0.0034	-0.0028
2.09	0.0000	0.0007	0.0032	-0.0030
2.53	0.0000	0.0007	0.0028	-0.0029
2.99	0.0000	0.0007	0.0032	-0.0029
3.81	0.0000	0.0007	0.0033	-0.0031
4.12	-0.0001	0.0008	0.0033	-0.0031
4.67	-0.0002	0.0007	0.0024	-0.0033
5.13	-0.0003	0.0008	0.0030	-0.0034
5.46	-0.0003	0.0008	0.0027	-0.0037
5.97	-0.0003	0.0008	0.0029	-0.0034
6.47	-0.0004	0.0008	0.0033	-0.0038
6.90	-0.0004	0.0008	0.0027	-0.0039
7.35	-0.0004	0.0008	0.0038	-0.0043
7.74	-0.0004	0.0009	0.0034	-0.0041
8.27	-0.0005	0.0008	0.0029	-0.0042
8.81	-0.0005	0.0010	0.0043	-0.0046
9.24	-0.0005	0.0008	0.0029	-0.0036
9.68	-0.0005	0.0009	0.0036	-0.0046
10.17	-0.0005	0.0010	0.0035	-0.0043
10.50	-0.0005	0.0010	0.0034	-0.0050
10.97	-0.0005	0.0013	0.0040	-0.0051
11.45	-0.0005	0.0015	0.0044	-0.0058
11.81	-0.0005	0.0012	0.0045	-0.0052
12.29	-0.0004	0.0014	0.0049	-0.0052
12.82	-0.0005	0.0014	0.0043	-0.0059
13.63	-0.0005	0.0017	0.0059	-0.0069
14.48	-0.0005	0.0020	0.0064	-0.0072
15.40	-0.0006	0.0024	0.0078	-0.0093
16.23	-0.0006	0.0018	0.0064	-0.0075

Figure D.22: Heaving response of configuration 4 (two walkways). Low turbulent flow. Structural damping: approx. 1.9% LD. n is the heaving frequency.

D.7.2 Torsional vibrations – 1.4% damping
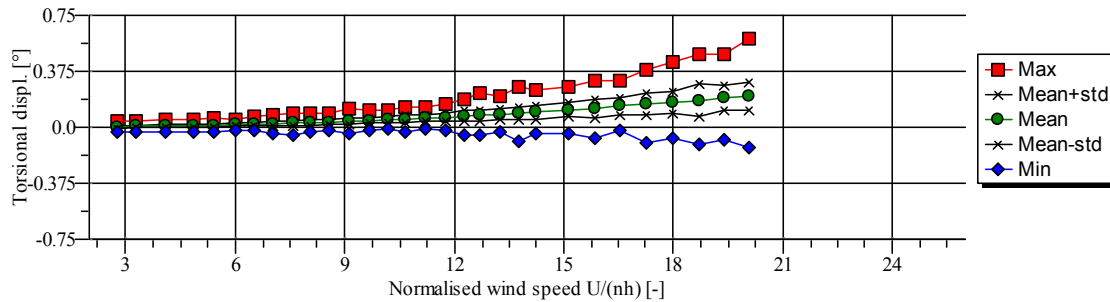
$U/(n_T h)$ [-]	Torsional displacement, Φ [°]			
	Mean	Std	Max	Min
2.78	0.0030	0.0086	0.0375	-0.0291
3.30	0.0052	0.0086	0.0422	-0.0282
4.11	0.0082	0.0092	0.0488	-0.0292
4.87	0.0117	0.0096	0.0503	-0.0284
5.42	0.0139	0.0110	0.0580	-0.0268
6.00	0.0173	0.0107	0.0564	-0.0209
6.53	0.0214	0.0117	0.0687	-0.0223
7.05	0.0246	0.0183	0.0883	-0.0397
7.58	0.0277	0.0183	0.0892	-0.0477
8.07	0.0319	0.0175	0.0937	-0.0324
8.55	0.0352	0.0162	0.0901	-0.0244
9.13	0.0408	0.0237	0.1264	-0.0388
9.66	0.0454	0.0185	0.1172	-0.0218
10.19	0.0507	0.0198	0.1169	-0.0131
10.66	0.0559	0.0267	0.1402	-0.0294
11.21	0.0616	0.0217	0.1370	-0.0113
11.76	0.0674	0.0285	0.1609	-0.0194
12.26	0.0742	0.0362	0.1918	-0.0530
12.69	0.0797	0.0362	0.2260	-0.0573
13.24	0.0874	0.0363	0.2119	-0.0324
13.74	0.0947	0.0443	0.2750	-0.0973
14.24	0.1014	0.0467	0.2535	-0.0456
15.13	0.1158	0.0471	0.2704	-0.0372
15.85	0.1263	0.0586	0.3143	-0.0730
16.56	0.1407	0.0536	0.3141	-0.0211
17.25	0.1521	0.0721	0.3852	-0.1079
17.98	0.1675	0.0757	0.4377	-0.0768
18.69	0.1814	0.1068	0.4919	-0.1179
19.38	0.1970	0.0872	0.4897	-0.0820
20.06	0.2108	0.0963	0.5933	-0.1396

Figure D.23: Torsional response of configuration 4 (two walkways). Low turbulent flow. Structural damping: approx. 1.4% LD. n is the torsional frequency.

**ASKØY BRIDGE
Wind tunnel tests and analyses**

Annex E

Wind tunnel

Contents in Annex E

E.1 The wind tunnel

The wind tunnel testing has been conducted in a boundary layer wind tunnel at Svend Ole Hansen ApS. The wind tunnel has a cross section of 1.55 x 1.75 m^2 as shown in Figure E.1.

A fan located at the beginning of the wind tunnel forces the flow through the wind tunnel, which is then guided back outside the wind tunnel by using vertical guide vanes after the test section. The maximum air velocity is approx. 10 m/s. However, by lowering the ceiling, it is possible to increase the maximum air velocity to approx. 16 m/s. Though, this is only used during calibration of measuring equipment as it would yield large blockage ratios during model testing.
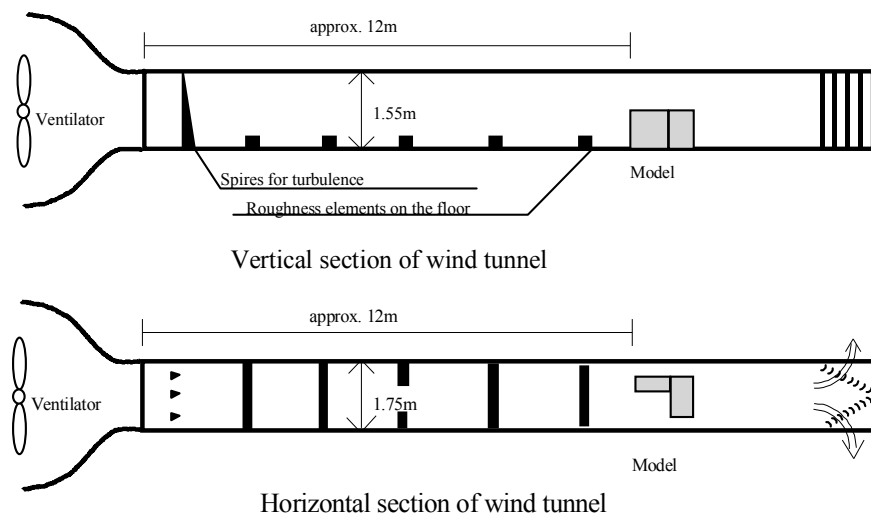
Figure E.1: Principle sketches of the boundary layer wind tunnel used in the testing.
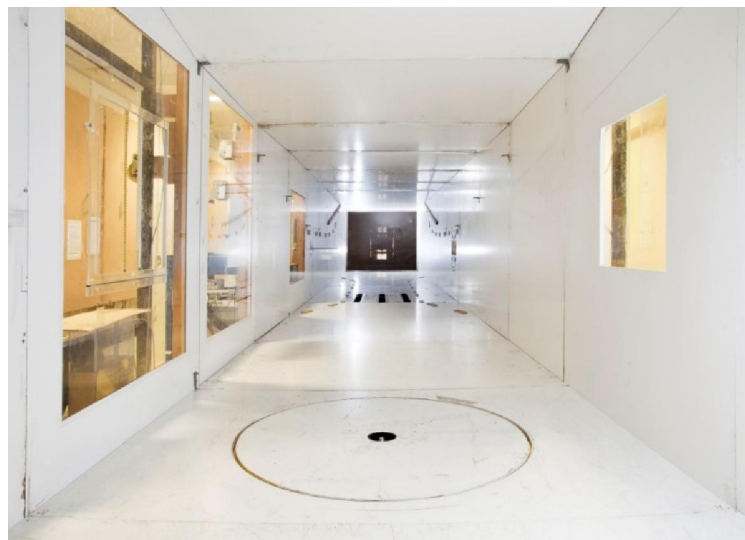
Figure E.2: Boundary layer wind tunnel at Svend Ole Hansen ApS. The picture shows the wind tunnel upstream.

Inside the wind tunnel, a Pitot tube is mounted approx. 0.3 m from the wall, 5 m upstream from the test position and 0.15 m below the test position. The Pitot tube measures both the static pressure and the stagnation pressure also known as the total pressure. The Pitot tube is connected to a manometer, which shows the dynamic pressure p_d found as the difference between the

stagnation pressure p_t and the static pressure p_s in accordance to Bernoulli's equation, see Equation (E.1).

$$p_t = p_s + p_d \qquad \text{(E.1)}$$

Hence, the air velocity can be determined by the definition of the dynamic pressure shown in Equation (E.2).

$$p_d = \frac{1}{2}\rho_{air}U^2 \Leftrightarrow U = \left(\frac{2p_d}{\rho_{air}}\right)^{0.5} \qquad \text{(E.2)}$$

This means that the air velocity is calculated by the air density ρ_{air}, which is a function of the barometric pressure and the temperature. The barometric pressure and the temperature is measured simultaneously with the dynamic pressure.

E.2 Flow properties

The distance from the contraction to the test section is approx. 12 m. In low turbulent flow, the distance between the contraction and test section is kept as smooth as possible, meaning no spires nor lists are mounted.

The turbulent boundary layer is created by placing three vertical spires right after the contraction and five lists on the floor between the contraction and the test section. The size of the spires and lists depends on the degree of turbulence intensity which is desired.

The roughness specified in the Danish and European norms can be modeled in the usual scales by using standardized test setups.

The horizontal velocity profile illustrating the horizontal homogeneity of the flow at the test position is shown in Figure E.3 for low turbulent flow. It is seen in Figure E.3 that close to the sides there is a boundary layer with a width of approx. 0-0.2 m where the air velocity is lower than in the center. The variation of the mean air velocity is within approx. 1.5 % in low turbulent flow.
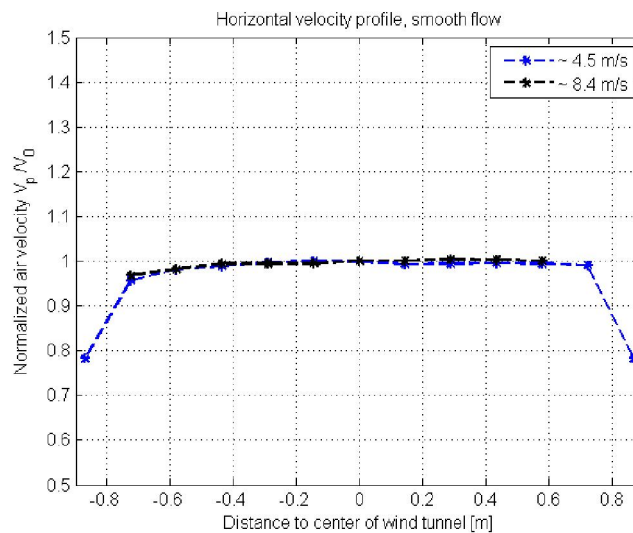
Figure E.3: Horizontal velocity profile. The blue line shows the velocity profile at 4.5 m/s while the black line shows the velocity profile at 8.4 m/s. V_0 is the air velocity at the center of the wind tunnel and V_p is the air velocity at other distances.

The ratio of the air velocity pressure along the model and the air velocity pressure at the Pitot tube is shown in Table E.1. Measurements have shown that the ratio of the velocity pressure at the model and the velocity pressure at the Pitot tube is independent of the air velocity in the range of velocities investigated in the present tests.

Table E.1: Ratio of mean velocity pressure q along the test position and the velocity pressure at the monitoring Pitot tube q_{pitot}.

	Smooth flow	Turbulent flow (13-15%)
q/q_{pitot}	1.02	1.05

E.3 The model

Model scales are typically chosen based on two contradicting criteria. On one hand, the model is desired to be as large as possible in order to model important details of the construction. However, due to the limited size of the wind tunnel, a too large model would cause blockage in the wind tunnel, which could have significant effects on the test results if the blockage ratio is above 5-10 %. The blockage ratio is defined as the projected area relative to the cross-sectional area of the wind tunnel which is 2.7 m^2.

E.3.1 Effect of scaling

Generally, it is expected that loads induced by a fluid flow around a body are determined by the established flow field around the body. The characterization of the flow field is the forces inside the fluid, such as the friction and inertia forces, acting on the surface of the body. If the ratio between all the acting forces are identical in both full and model scale, the two flows can be considered being similar to each other, meaning *full physical similarity* is achieved. However, in practice it is not necessary to match every full scale force to the model. When basing the similarity of the ratios of e.g. Reynolds number and the ratio between inertia and viscous forces related to flow states or properties *fluid mechanical similarity* is achieved. This covers the majority of physical phenomena in connection to flow-induced load and responses.

Though, fluid mechanical similarity is not possible to simulate in wind tunnel testing as the physical properties of the air are identical in both nature and wind tunnel testing. Likewise, the gravity of the earth is a natural constant and invariable through all scales. This means only *partial similarity* is achieved allowing a certain degree of scaling mismatch on secondary flow phenomena.

Another criterion for similarity is the similarity of the flow field geometry and acting forces in nature and in model scale. This assumption is based on the fact that a specific unique ratio of all acting forces will create a corresponding specific unique flow field, giving an identical flow pattern and hence identical force ratios. Analyzing the geometry of a flow field, it is obvious that in model scale, two related flow fields need to be taken care of, namely the background and the near flow around the body. The properties of the background flow are generally described by the airflow distribution of mean air velocity, turbulence intensity, coherence and integral length scale of the turbulence, while the near field of the flow around a body is characterized by stagnation, separation and reattachment of the flow on the body. Typically, one can assume that the background flow is properly scaled, meaning the near flow around the body needs proper scaling. This can be done by Reynolds law, which specifies identical ratios between inertial and friction forces in model scale (*MS*) and in nature (*FS*) as shown in Equation (E.3):

$$\frac{F_{I_{MS}}}{F_{\mu_{MS}}} = \frac{F_{I_{FS}}}{F_{\mu_{FS}}} \implies \frac{1/2\rho_{MS}U_{MS}^2 A_{MS}}{\mu_{MS}\frac{\partial U_{MS}}{\partial y_{MS}}A_{MS}} = \frac{1/2\rho_{FS}U_{FS}^2 A_{FS}}{\mu_{FS}\frac{\partial U_{FS}}{\partial y_{FS}}A_{FS}} \Longleftrightarrow$$

(E.3)

$$\frac{\rho_{MS}U_{MS}L_{MS}}{\mu_{MS}} = \frac{\rho_{FS}U_{FS}L_{FS}}{\mu_{FS}} \Longleftrightarrow \frac{U_{MS}L_{MS}}{\nu_{MS}} = \frac{U_{FS}L_{FS}}{\nu_{FS}} \Longleftrightarrow Re_{MS} = Re_{FS}$$

where

F_I is inertial forces

F_μ is friction forces

U is the air velocity

A is the area

μ is the dynamic viscosity

$\dfrac{\partial v}{\partial y}$ is the velocity gradient near a body with the distance y

L is the length

v is the kinematic viscosity

Due to the fact that the physical properties of air is the same in both nature and model, it would as a consequence of the Reynolds law require extreme model air velocities in order to fulfill the law. In the present case, the geometric scale is 1:25, meaning it would require 25 times the presumed full-scale wind speed to fulfill the Reynolds law. This is most often not possible to simulate and could therefore lead to a change of the separation points compared to the nature and hence a significant error in the results.

When a fluid approaches a body, the area around the body becomes a region consisting of disturbed flow. This disturbance in the flow is caused by the separation of the local surface boundary layer at some point along the body. This leads to a change in the flow, going from moving in streamlines in smooth flow into an unsteady flow in different directions. Typically, bodies are distinguished between rounded and sharp-edged bodies. On sharp-edged bodies, the location of the separation point is predefined by the location of the sharp edges while on rounded bodies, which have no sharp edges, the separation point varies depending on the air velocity and thus Reynolds number Re. At $Re > 40$ the separation of the boundary layer over the cylinder is caused by an adverse pressure gradient, which is imposed by the divergent geometry of the flow environment at the rear side of the cylinder. This causes the formation of a shear layer as shown in Figure E.4.
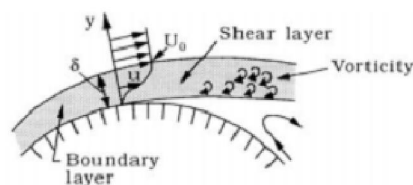
Figure E.4: Detailed figure of flow near separation [5].

The change of separation point with Reynolds number on rounded bodies means that the forces might be overestimated when scaling rounded bodies from full-scale to model scale. However, for sharp-edged bodies a relaxation within Reynolds scaling can be allowed as the separation points are predefined by the body geometry and are therefore independent of the air velocity and the Reynolds number provided that separation occurs. Additionally, the reattachment points can be assumed to be correct if the following is fulfilled:

$$Re = \frac{U\,L}{v} > Re_{ons} = 4000 \tag{E.4}$$

where

Re_{ons} is the onset Reynolds number for invariant flow field geometry

Fulfilling the requirement presented in Equation (E.4), the ratios for geometry, frequency, time and velocity between model and full scale are:

Geometric scale	$\lambda_L = \dfrac{L_{MS}}{L_{FS}}$
Frequency scale	$\lambda_F = \dfrac{f_{MS}}{f_{FS}}$
Time scale	$\lambda_T = \dfrac{1}{\lambda_F}$
Velocity scale	$\lambda_U = \dfrac{\lambda_T}{\lambda_L}$

ASKOY BRIDGE

Wind tunnel tests and analyses

Annex F

Received information

Contents in Annex F

F.1 GANGBANE ASKØYBRUA REV03

The information on which the wind tunnel tests are based is included in the present annex. Drawings have not been included.